# The golgin protein Coy1 functions in intra-Golgi retrograde transport and interacts with the COG complex and Golgi SNAREs

Nadine S. Anderson, Indrani Mukherjee, Christine M. Bentivoglio, and Charles Barlowe*
Department of Biochemistry & Cell Biology, Geisel School of Medicine at Dartmouth, Hanover, NH 03755

**ABSTRACT** **Extended coiled-coil proteins of the golgin family play prominent roles in maintaining the structure and function of the Golgi complex. Here we further investigate the golgin protein Coy1 and document its function in retrograde transport between early Golgi compartments. Cells that lack Coy1 displayed a reduced half-life of the Och1 mannosyltransferase, an established cargo of intra-Golgi retrograde transport. Combining the *coy1Δ* mutation with deletions in other putative retrograde golgins (*sgm1Δ* and *rud3Δ*) caused strong glycosylation and growth defects and reduced membrane association of the conserved oligomeric Golgi (COG) complex. In contrast, overexpression of *COY1* inhibited the growth of mutant strains deficient in fusion activity at the Golgi (*sed5-1* and *sly1-ts*). To map Coy1 protein interactions, coimmunoprecipitation experiments revealed an association with the COG complex and with intra-Golgi SNARE proteins. These physical interactions are direct, as Coy1 was efficiently captured in vitro by Lobe A of the COG complex and the purified SNARE proteins Gos1, Sed5, and Sft1. Thus our genetic, in vivo, and biochemical data indicate a role for Coy1 in regulating COG complex-dependent fusion of retrograde-directed COPI vesicles.**

**Monitoring Editor**
Akihiko Nakano
RIKEN

Received: Mar 3, 2017
Revised: Jul 12, 2017
Accepted: Jul 31, 2017

## INTRODUCTION

Nascent secretory proteins that have been glycosylated and folded in the endoplasmic reticulum (ER) are delivered to the *cis*-Golgi in a coat protein complex II– (COPII) dependent manner (Brandizzi and Barlowe, 2013; Xu and Ng, 2015). As glycosylated secretory proteins traverse the Golgi, they are sequentially subjected to a series of glycan trimming, extension, and modification reactions. The order of these reactions arises from the compartmentalization of the Golgi, wherein each cisterna is enriched in a distinct set of resident enzymes, transporters, and chaperones (Stanley, 2011). Maintenance of compartmental identity requires that resident Golgi proteins are localized to the correct cisterna, yet many of these proteins are not statically retained to one cisterna (Harris and Waters, 1996; Todorow *et al.*, 2000). Instead, resident proteins flow forward through the Golgi and are recycled back to earlier compartments through a vesicular trafficking pathway referred to as intra-Golgi retrograde transport (Banfield 2011; Fisher and Ungar, 2016).

Early Golgi resident proteins that have flowed to later cisternae are first packaged into coat protein complex I (COPI)-coated vesicles in an Arf1- and Vps74-dependent manner (Lanoix *et al.*, 2001; Martínez-Menárguez *et al.*, 2001; Tu *et al.*, 2008). These vesicles are then directed to specific Golgi compartments by Rab GTPases (Mizuno-Yamasaki *et al.*, 2012) and a subset of coiled-coil proteins known as golgins (Gillingham and Munro, 2016). Once tethered to the appropriate membrane, the vesicular Qc-SNARE Sft1 bundles together with the cisternal Qa-, Qb-, and R-SNAREs Sed5, Gos1, and Ykt6 to drive fusion between the opposing membranes (Bock *et al.*, 2001; Parlati *et al.*, 2002; Xu *et al.*, 2002; Volchuk *et al.*, 2004). Both the tethering and fusion steps depend on the conserved oligomeric Golgi (COG) complex, a member of the multi-subunit CATCHR-family of transport factors (Yu and Hughson, 2010; Climer *et al.*, 2015). Although these components have been well characterized individually, it remains mechanistically unclear how, when, and where they are coordinated with one another to orchestrate vesicle capture and fusion.

This article was published online ahead of print in MBoC in Press (http://www.molbiolcell.org/cgi/doi/10.1091/mbc.E17-03-0137) on August 9, 2017.

*Address correspondence to: Charles Barlowe (charles.barlowe@dartmouth.edu).

Abbreviations used: COG, conserved oligomeric Golgi; COPI, coat protein complex I; COPII, coat protein complex II; HA, hemagglutinin tag; SNARE, soluble NSF attachment protein receptor.

Here we report a role for Coy1 in intra-Golgi retrograde transport. Coy1 has been implicated in this transport process based on a genetic interaction between *COY1* and *gos1Δ*. Both *COY1* and its human homologue *CASP* encode a ~75-kDa Golgi-localized protein with a C-terminal transmembrane domain and a cytoplasmic N-terminus composed of a series of coiled coils (Gillingham *et al.*, 2002). CASP has been proposed to function as a tether for retrograde-directed Golgi vesicles, as recombinant CASP could specifically capture vesicles laden with resident Golgi enzymes (Malsam *et al.*, 2005). However, CASP was unable to nucleate vesicle tethering events in vivo when targeted to an ectopic site (Wong and Munro, 2014). Thus the functions of CASP and Coy1 remain enigmatic.

The identification of Coy1 as a COPII vesicle protein led us to further investigate its role in the early secretory pathway (Margulis *et al.*, 2016). Here we report that Coy1 has no direct effect on ER to Golgi transport in a cell-free transport assay. Instead, our live cell labeling, genetic, and biochemical studies indicate a role for Coy1 in intra-Golgi retrograde transport. Rather than a function in tethering as has been established for most other golgins, our genetic and physical interactions implicate Coy1 in organizing the cisternal Golgi membrane for fusion with incoming retrograde directed vesicles.

## RESULTS

### Coy1 in ER-Golgi transport

We previously identified Coy1 as an enriched component of COPII vesicles in proteomic analyses (Margulis *et al.* 2016). To validate this result, a small-scale COPII budding reaction was conducted (Barlowe *et al.*, 1994). Microsomes derived from wild-type (WT) cells were incubated with an energy regeneration system and purified COPII proteins to drive vesicle budding. Vesicles were separated from bulk membranes by centrifugation, and samples of the vesicular fraction were compared with the reaction input by immunoblotting (Figure 1A) (Belden and Barlowe 1996). The ER vesicle protein Erv41 was enriched in the COPII vesicle fraction as previously reported (Otte *et al.*, 2001), as was Coy1. A subunit of the translocon, Sec63, was not detectable in the vesicular fraction (Feldheim *et al.* 1992). The distributions of Erv41 and Sec63 were unchanged in the *coy1Δ* strain. Thus Coy1 is efficiently packaged into COPII vesicles but has no apparent effect on COPII packaging efficiency or stringency.

We wondered whether Coy1 served as a vesicular tether that initiates contact between COPII vesicles and the *cis*-Golgi. To test this possibility, we monitored anterograde ER-Golgi transport in wild-type and *coy1Δ* strains using a cell-free assay (Cao *et al.*, 1998). Overall transport (Figure 1B) and tethering (Figure 1C) efficiency in *coy1Δ* were indistinguishable from the wild-type reactions. As tethering factors at the Golgi are predicted to exhibit some functional redundancy with one another (Munro 2011; Roboti *et al.* 2015; Gillingham and Munro 2016), we hypothesized that a transport defect would become apparent if *COY1* was deleted in addition to other golgins implicated in ER to Golgi transport. We repeated the transport assay using strains lacking Coy1 and either of the putative ER to Golgi tethering factors, Rud3 or Grh1 (VanRheenen *et al.*, 1999; Behnia *et al.*, 2007). No change in transport efficiency was observed in a *coy1Δ rud3Δ* double mutant (data not shown). Strikingly, a tethering defect apparent in *grh1Δ* membranes (Behnia *et al.*, 2007) was suppressed by combining with *coy1Δ* (Figure 1D), suggesting Coy1 can indirectly affect anterograde transport despite being dispensable for this process. Consistent with this interpretation, overexpression of *COY1* was

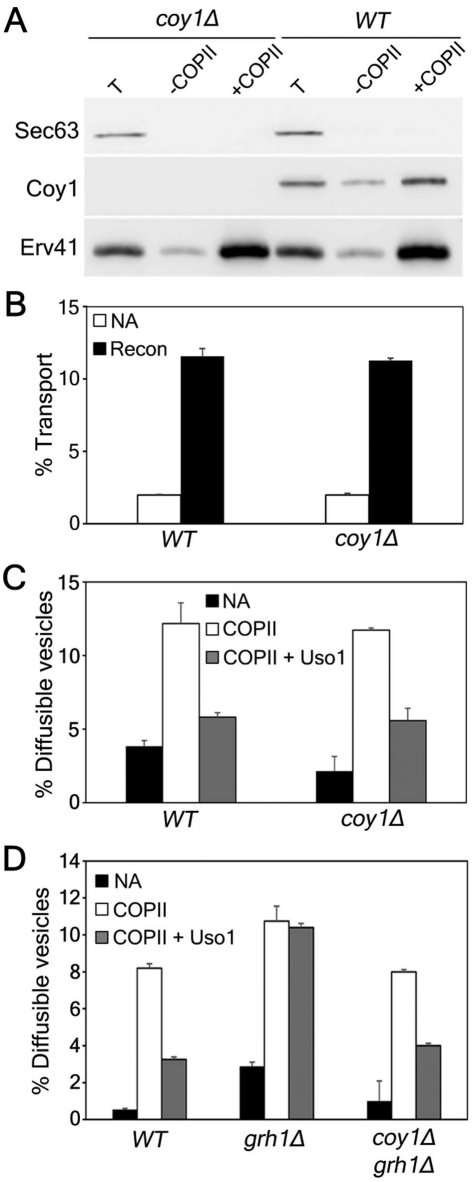


**FIGURE 1:** Coy1 is not required for anterograde transport. (A) Washed semi-intact cells from wild-type (CBY740) and *coy1Δ* (CBY2660) strains were incubated with or without purified COPII proteins to monitor vesicle budding. Ten percent of the total membrane input (T) and the vesicular fractions were resolved on 10.5% SDS–PAGE gels and immunoblotted using antibodies against Sec63 (as a negative control), Erv41 (as a positive control), and Coy1. (B) In a cell-free ER to Golgi transport assay, membranes were loaded with [$^{35}$S]gpαf, washed, and incubated at 23°C for 1 h with an ATP regeneration system and the absence (NA) or presence (Recon) of purified COPII, Uso1, and LMA1. The percentage of [$^{35}$S]gpαf that had received α1,6 modification was quantified as a readout of transport efficiency. (C) Tethering assays were conducted by incubating WT and *coy1Δ* membranes at 23°C for 30 min with an ATP regeneration system and either no addition (NA), purified COPII proteins or purified COPII and Uso1. Samples were then centrifuged to separate bulk membranes from diffusible vesicles. The percentage of protease resistant [$^{35}$S]gpαf remaining in the vesicular fraction was measured as a readout of tethering efficiency. (D) Tethering assays were conducted as described in C with membranes prepared from WT (CBY740), *grh1Δ* (CBY3178), *or coy1Δ grh1Δ* (CBY3258) strains. Tethering efficiency was 71% in the WT strain, 12.5% in *grh1Δ*, and 58% in *coy1Δ grh1Δ*.

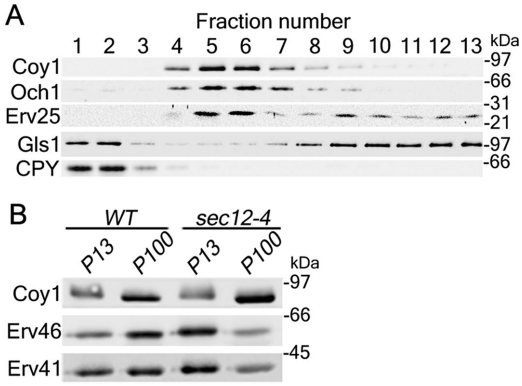


**FIGURE 2:** Coy1 is localized to Golgi membranes. (A) Cell lysate from a WT (CBY740) strain was centrifuged through a 18–60% sucrose density gradient. Fractions were collected from the top to the bottom of the gradient and resolved on 10.5% SDS–PAGE gels. Immunoblotting was conducted with polyclonal antibodies against the early Golgi mannosyltransferase Och1, the ER vesicle protein Erv25, the ER glucosidase Gls1, the vacuolar hydrolase CPY, and Coy1. (B) WT and *sec12-4* strains were grown to early log phase at 25°C and treated with 50 µg/ml cycloheximide for 20 min to halt translation. The cultures were then shifted to 38.5°C for 90 min to induce an ER export block in *sec12-4* cells. After conversion to spheroplasts, cell lysates were centrifuged to generate ER (p13)- and Golgi (p100)-enriched membrane pellets. The membrane pellets were solubilized and separated on 10.5% SDS–PAGE gels. Immunoblotting was conducted with antiserum against Coy1, as well as Erv41 and Erv46, both of which actively cycle between the Golgi and ER.

sufficient to induce transport and tethering defects (Supplemental Figure 1).

### Coy1 distribution and trafficking

To understand how Coy1 could exert such an effect on anterograde transport, we sought to characterize the protein more thoroughly, beginning with investigating its localization and trafficking pattern. Coy1 colocalizes with a *cis*-Golgi marker via immunofluorescence microscopy (Gillingham *et al.*, 2002), but its precise subcellular distribution is unknown. To address this question, membranes from wild-type cell lysates were resolved on sucrose gradients (Figure 2A). The hydrolase carboxypeptidase Y (CPY) was present exclusively in the vacuolar fractions. Most of the glucosidase Gls1 was present in ER fractions, with a secondary peak cofractionating with CPY, consistent with prior reports showing that a low level of Gls1 leaks to later secretory pathway compartments (Shibuya *et al.*, 2015). The ER vesicle protein Erv25 exhibited a split distribution between ER fractions and Golgi fractions as previously observed (Belden and Barlowe, 1996, 2001). Only trace amounts of Coy1 were present in the ER fractions, with the bulk of this protein cofractionating with Och1, the Golgi-resident mannosyltransferase that initiates addition of α1,6-mannose residues to the core oligosaccharide of nascent secretory proteins (Nakanishi-Shindo *et al.*, 1993; Brigance *et al.*, 2000). By both fluorescence microscopy and sucrose gradient sedimentation, Coy1 is almost exclusively Golgi localized.

A subset of resident Golgi proteins cycle back to the ER from the Golgi (Todorow *et al.*, 2000). Resident Golgi proteins that do not actively traffic back to the ER have been proposed to serve as structural components of the Golgi complex (Seemann *et al.*, 2000). CASP belongs to the latter category of resident Golgi proteins, as CASP remains Golgi localized when an ER export block is induced in BSC-1 cells by microinjection of a dominant-negative form of Sar1 (Malsam *et al.*, 2005). To determine whether Coy1 undergoes Golgi to ER retrograde transport or whether it remains Golgi-localized like CASP, wild-type and *sec12-4* cells were grown to early-log phase at a permissive temperature, treated with cycloheximide to purge the secretory pathway of newly synthesized proteins, and shifted to a restrictive temperature of 38.5°C to induce an ER export block (Todorow *et al.*, 2000). Under this condition, cycling proteins should be trapped in the ER. Cells were then lysed and differentially centrifuged to prepare ER- and Golgi-enriched membrane pellets (Belden and Barlowe, 2001). Two proteins known to actively cycle between the Golgi and ER, Erv41 and Erv46, exhibited a split distribution between these two fractions in wild-type cells (Shibuya *et al.*, 2015) and redistributed to the ER fraction in the *sec12-4* strain (Figure 2B). In contrast, the distribution of Coy1 was unchanged between the wild-type and *sec12-4* conditions. The apparent molecular weight of Coy1 was reduced in the Golgi fractions relative to those in the ER, perhaps indicating compartment-specific posttranslational modifications, e.g., phosphorylation (Albuquerque *et al.*, 2008; Holt *et al.*, 2009; Swaney *et al.*, 2013), but this observation was not pursued further. This result indicates that Coy1, like its mammalian homologue CASP, is enriched at the Golgi and does not actively traffic back to the ER. As Coy1 does not cycle back to the ER from the Golgi and is not necessary for anterograde transport, we conclude that the enrichment of Coy1 on COPII vesicles likely reflects its biosynthetic route for delivery to Golgi membranes.

Most golgins possess a C-terminal motif required for their localization at the Golgi (reviewed in Gillingham and Munro, 2016). The C-terminal transmembrane domain of Coy1 presumably directs this protein to the Golgi, but it has not been directly tested if this region is necessary and sufficient for Golgi localization of Coy1. To address this possibility, endogenous *COY1* was truncated and the hemagglutinin (HA) epitope inserted by gene targeting just prior to the region encoding the transmembrane domain (Longtine *et al.*, 1998), and the localization of the Coy1 protein was then examined by immunofluorescence microscopy (Figure 3, A and B). Coy1-HA and Coy1ΔTM-HA exhibited a punctate distribution typical of Golgi proteins. The Coy1 puncta partially overlapped with Och1 in both the HA-tagged strains (Figure 3A). Incomplete colocalization of Coy1 with Och1 suggests that Coy1 does not exclusively reside on early Golgi compartments. No substantial colocalization was observed between Coy1 and the ER resident protein Kar2 in either of these strains (Figure 3, A and B). As a complementary approach, the subcellular distribution of Coy1 from wild-type and Coy1ΔTM-HA cells was investigated by fractionation on sucrose gradients. In the wild-type strain, 95% of Coy1 cofractionated with Och1, while 5% was detected in the ER, likely reflecting newly synthesized Coy1 (Figure 3C). Although Coy1ΔTM-HA cofractionation with Och1 was reduced to an average of 70% in a set of replicates, the protein remained clearly enriched in the Golgi fractions relative to the vacuolar and ER fractions (both of which had ~15% of total Coy1ΔTM-HA). We next examined the functionality of Coy1ΔTM-HA through a set of genetic approaches. Overexpression of both Coy1 and Coy1ΔTM-HA under the control of the *GAL* promoter was sufficient to induce growth defects in a wild-type background (Supplemental Figure 2A). However, a strain that requires Coy1 to survive on media containing calcofluor white (described in the following section) was unable to grow when supplemented with a plasmid encoding Coy1ΔTM-HA (Supplemental Figure 2B), indicating that although Coy1 and Coy1ΔTM-HA can both impair growth when highly overexpressed, Coy1ΔTM-HA cannot functionally replace the endogenous protein. As the transmembrane domain is partially dispensable for Golgi localization, we conclude that the transmembrane domain exerts a function beyond simply serving as a membrane anchor for Coy1.

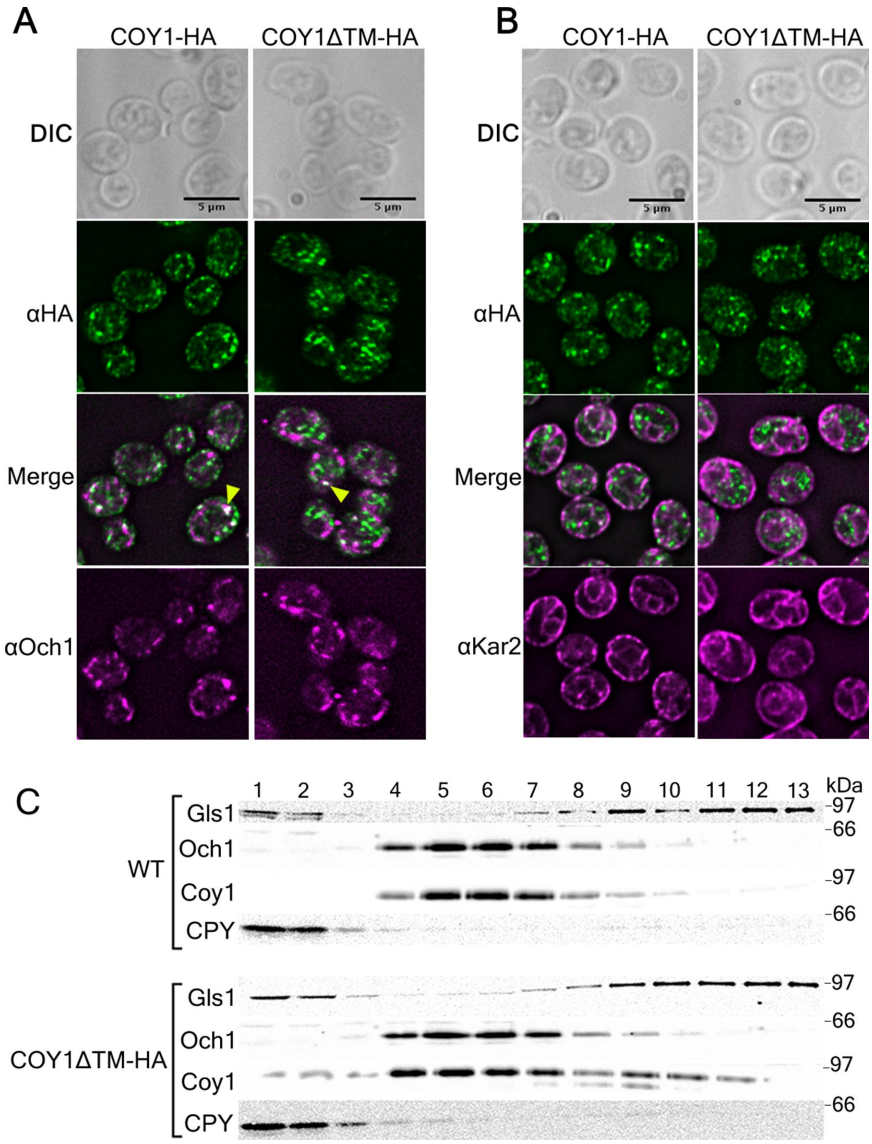


**FIGURE 3:** The transmembrane domain of Coy1 is dispensable for Golgi enrichment. (A) Localization of Coy1-HA (CBY2674) and Coy1ΔTM-HA (CBY3484) in cells was examined by immunofluorescence microscopy using monoclonal antibodies against the HA epitope and polyclonal antibodies against the Golgi mannosyltransferase Och1. Yellow arrowheads point to sites of colocalization. Scale bars represent 5 μm. (B) Costaining was performed as in A with monoclonal antibodies against the HA epitope and with polyclonal antibodies against the ER chaperone Kar2. (C) Spheroplasts from wild-type (CBY740) and Coy1ΔTM-HA (CBY3484) cells were separated on a sucrose gradient as in Figure 2A. Samples from each fraction were resolved on 10.5% SDS–PAGE gels and immunoblotted using polyclonal antibodies against Gls1, Coy1, Och1, and CPY.

### Coy1 functions in intra-Golgi transport

As Coy1 is dispensable for ER to Golgi anterograde transport in vitro and does not actively cycle back to the ER for a role in Golgi to ER retrograde transport, we wondered if Coy1 instead functioned in intra-Golgi retrograde transport. CASP has been implicated in this transport process, as microinjection of soluble, recombinant CASP inhibits intra-Golgi retrograde transport of the Golgi enzyme GalNAcT2-YFP (Malsam *et al.*, 2005). We tested if Coy1 might contribute to this transport process by examining the retention of an established cargo of intra-Golgi retrograde transport, Och1, by pulse-chase analysis (Harris and Waters, 1996; Bruinsma *et al.*, 2004). Wild-type and *coy1Δ* cells were pulsed with a mix of radiolabeled [$^{35}$S]cysteine/[$^{35}$S]methionine and then chased with an excess of unlabeled amino acids. Lysates from each time point were immunoprecipitated using antiserum against Och1 and a control protein, Kar2. Kar2 levels remained comparable throughout the chase period in both strains (Figure 4, bottom panel). By the end of the chase, Och1 levels were slightly reduced in the wild-type strain, whereas Och1 was rapidly depleted in the *coy1Δ* strain (Figure 4). The difference in the half-life of Och1 between the two strains was statistically significant ($p < 0.05$, unpaired Student's *t* test). We interpret this to indicate an Och1 retention defect in *coy1Δ,* resulting in missorting and degradation of Och1.

As Och1 initiates outer-chain mannose extension, one might expect a defect in the retention of this enzyme to result in hypoglycosylation. However, no such glycosylation defects are apparent in *coy1Δ* cells, and total Och1 protein levels are similar between wild-type and *coy1Δ* cells (data not shown). We wondered if such a phenotype was being buffered against by other redundant transport components. Three mammalian golgins, GMAP-210, TMF, and golgin-84, are sufficient to initiate capture of vesicles laden with resident Golgi proteins in vivo (Wong and Munro 2014). The former two golgins have orthologues in yeast, called Rud3 and Sgm1, that have also been implicated in retrograde Golgi transport (Kim *et al.*, 1999; VanRheenen *et al.*, 1999; Siniossoglou and Pelham, 2001; Kim, 2003). If Coy1 functions in this process alongside Rud3 and Sgm1, cells could exhibit growth and glycosylation defects as more of these golgins are lost. To test this possibility, serial dilution assays were conducted using strains lacking one, two, or all three of these golgins (Figure 5A). No apparent phenotype was observed in *coy1Δ rud3Δ,* consistent with prior reports (Gillingham *et al.*, 2002), while a mild growth defect was apparent in *coy1Δ sgm1Δ*. A more severe phenotype was observed in *rud3Δ sgm1Δ*. The triple knockout grew similarly to *rud3Δ sgm1Δ* at lower temperatures but was completely unable to grow at the restrictive temperature (Figure 5A). Expression of *COY1* on a plasmid was sufficient to suppress this phenotype (Supplemental Figure 2C). These results indicate that *COY1* is required for viability at high temperatures when *RUD3* and *SGM1* are both absent.

A similar pattern of growth was observed when the same strains were grown in the presence of calcofluor white, a cell wall stressor used to identify glycosylation mutants (Ram *et al.*, 1994). The *rud3Δ* strain exhibited mild sensitivity to calcofluor white (Figure 5B), whereas the *coy1Δ* and *sgm1Δ* strains were not affected. The *coy1Δ sgm1Δ* mutant exhibited a growth defect on media containing calcofluor white, as did the *rud3Δ sgm1Δ* strain. The triple knockout

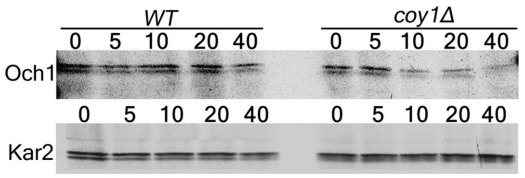


FIGURE 4: The half-life of the Golgi mannosyltransferase Och1 is reduced in *coy1Δ* cells. Early log phase cultures of wild-type (CBY740) or *coy1Δ* (CBY2660) cells were pulsed with a radiolabeled cysteine/methionine mix and then chased with an excess of unlabeled amino acids. Samples were taken at the indicated time points and were subsequently lysed and then proteins were immunoprecipitated with antibodies against Och1 or Kar2. Immunoprecipitates were resolved on 10.5% SDS–PAGE gels and visualized by autoradiography. The half-life of Och1 was quantified from three independent experiments. In the wild-type strain, the half-life of Och1 was 98.5 min with a SD of 10.1, while the half-life of Och1 in *coy1Δ* was 40.3 (+/– 27.9, $n = 3$).

failed to grow at any temperatures beyond the first dilution. Viability of the triple knockout on media with calcofluor white was restored when *COY1* was provided on a plasmid. Notably, a plasmid encoding Coy1ΔTM failed to rescue growth of this strain, indicating that the transmembrane domain of Coy1 is functionally important (Supplemental Figure 2B). These results suggested that glycosylation defects become exacerbated as more of these golgins are lost. To validate this interpretation, the glycoproteins Gas1 and CPY were examined in whole-cell lysates derived from each strain (Figure 5C). Gas1 exits the ER as a 105-kDa protein and is further glycosylated as it traverses the Golgi to a 120-kDa form (Fankhauser and Conzelmann, 1991). CPY exits the ER as a 67-kDa proprotein, is glycosylated in the Golgi to 69 kDa, and is proteolyzed in the vacuole to its mature 61-kDa form (Hasilik and Tanner, 1978; Stevens *et al.*, 1982). The molecular weight of Gas1 was unchanged relative to the wild-type strain in each of the single knockouts but was reduced in the *coy1Δ sgm1Δ* and *rud3Δ sgm1Δ* double mutants. Notably, the

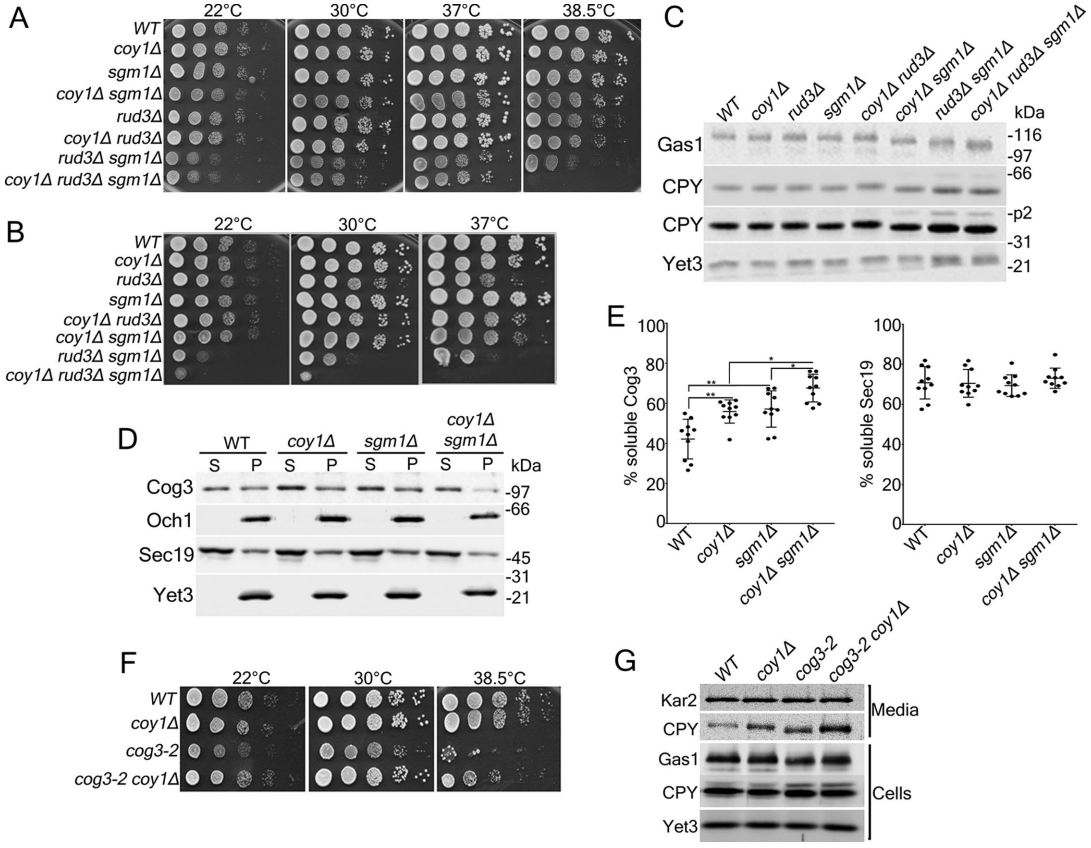


FIGURE 5: *COY1* genetically interacts with tethering factors involved in intra-Golgi retrograde transport. (A) Tenfold serial dilutions were set up on YPD plates at the indicated temperatures with the following strains: WT (CBY740), *coy1Δ* (CBY2660), *rud3Δ* (CBY2678), *sgm1Δ* (CBY3874), *coy1Δ sgm1Δ* (CBY4102), *coy1Δ rud3Δ* (CBY2692), *rud3Δ sgm1Δ* (CBY4101), *and coy1Δ rud3Δ sgm1Δ* (CBY4103). (B) Serial dilutions were set up as in A on YPD + 5 μg/ml Calcofluor White. (C) Lysates derived from midlog phase cultures of the indicated strains were separated on a 10% SDS–PAGE gel and immunoblotted for Gas1, CPY, and Yet3. A darker exposure of the CPY blot is also shown to highlight accumulation of the p2 precursor. (D) Semi-intact cells were centrifuged at 100,000 × g to resolve cytosolic proteins in the supernatant fraction (S) from membrane bound proteins in the pellet (P). Equivalent amounts of each sample were resolved on 11% SDS–PAGE gels and immunoblotted for Cog3, Och1, Sec19, and Yet3. (E) Quantification of the percentage of Cog3 and Sec19 present in the supernatant fraction as depicted in D (means ± SD, $n = 10$ independent experiments, $*p < 0.05$, $**p < 0.005$, one-way ANOVA followed by Tukey's test). (F) Wild-type (CBY740), *coy1Δ* (CBY2659), *cog3-2* (CBY3881), and *cog3-2 coy1Δ* (CBY4788) strains were diluted onto YPD plates at the indicated temperatures. (G) Cultures from F were grown to early-log phase at 30°C and then shifted to 38.5°C for 1 h. Cells were separated from the medium by centrifugation, and secreted proteins were concentrated by trichloroacetic acid (TCA) precipitation while cell lysates were prepared by bead-beating. Media and cellular proteins were resolved on 10.5% SDS–PAGE gels and immunoblotted for CPY and Gas1, with Kar2 and Yet3 serving as loading controls.

molecular weight of Gas1 was reduced further still in the triple knockout relative to the double mutants. CPY was also underglycosylated in lysates from the *coy1Δ sgm1Δ, rud3Δ sgm1Δ,* and *coy1Δ rud3Δ sgm1Δ,* with the latter two strains also exhibiting an accumulation of a precursor form of CPY, indicative of a transport defect. These results solidify a role for Coy1 in maintaining the fidelity of glycosylation, along with Rud3 and Sgm1.

We next sought to identify a mechanistic cause for these additive phenotypes. In a yeast two-hybrid assay, every identified mammalian golgin protein interacts with the COG complex (Miller *et al.*, 2013), an octameric peripheral membrane protein complex that is implicated in vesicle tethering and fusion throughout the Golgi (Fisher and Ungar, 2016). These interactions led us to test whether golgin proteins collectively function to recruit the COG complex to the Golgi membrane. We focused our analysis on *coy1Δ* and *sgm1Δ* because a strain carrying both mutations exhibited a glycosylation defect (Figure 5, B and C) and to avoid confounding effects caused by disrupted ER to Golgi trafficking that may arise from *rud3Δ*. Semi-intact cells derived from wild type, *coy1Δ*, *sgm1Δ,* and *coy1Δ sgm1Δ* cultures were diluted in buffer and centrifuged at 100,000 × *g* for 20 min to separate cytosol from cellular membranes. The integral membrane proteins Yet3 and Och1 were both solely detected in the membrane pellet fraction, while Sec19, a protein that cycles between membranes and the cytosol (Garrett *et al.*, 1994), was similarly enriched in the cytosol in each strain (Figure 5, D and E). Cog3 appeared equally split between the membrane and cytosolic fractions in the wild-type setting. This distribution significantly shifted toward the cytosol in the *coy1Δ* and *sgm1Δ* strains, and this redistribution was more pronounced in the *coy1Δ sgm1Δ* strain (Figure 5, D and E). Thus the glycosylation defect in the *coy1Δ sgm1Δ* strain can be partially attributed to disrupted COG complex membrane association.

Attenuated membrane association of the COG complex in the *coy1Δ* strain suggested an interaction between Coy1 and the COG complex. To address the physiological relevance of this potential interaction, a haploid strain lacking *COY1* and bearing the *cog3-2* point mutation was constructed by mating, and its growth was compared with that of the parent strains (Figure 5D). The *cog3-2* strain grows poorly at lower temperatures and is inviable at an elevated temperature (Wuestehube *et al.*, 1996). Strikingly, deletion of *COY1* suppressed this growth defect, and the double mutant remained viable at the restrictive temperature, although its growth was reduced relative to the wild-type and *coy1Δ* strains. Expression of *COY1* on a plasmid was sufficient to reintroduce a strong growth defect in the *cog3-2 coy1Δ* strain (Supplemental Figure 2D). However, the glycosylation and transport defects of *cog3-2* were not corrected, as Gas1 and CPY ran at a reduced molecular weight in cell lysates from both the *cog3-2* and *cog3-2 coy1Δ*, stains and an accumulation of p2 CPY was apparent in both strains as well. Furthermore, secretion of p2 CPY was elevated an average of 1.46 (± 0.17 SD, $n = 3$) and 1.37 (± 0.28)-fold relative to the wild-type strain in the *coy1Δ* and *cog3-2* single mutants and was elevated 2.3-fold (± 0.39) in the double mutant (Figure 5E). These results functionally implicate COG complex and Coy1 with one another but also indicate that the latter does not simply act as a negative regulator of the former.

The COG complex and Coy1 both affect SNARE function. The COG complex physically and functionally interacts with the early Golgi syntaxin Sed5 and its cognate SM protein Sly1 (Suvorova *et al.*, 2002; Shestakova *et al.*, 2007; Laufman *et al.*, 2009), while overexpression of *COY*1 results in a severe growth defect in a strain lacking the retrograde Golgi SNARE Gos1 (Gillingham *et al.*, 2002). We wondered whether these SNARE interactions could explain how *coy1Δ* suppresses the growth defect of *cog3-2*. We observed that overexpression of *COY1* was toxic in strains bearing either the *sed5-1* or *sly1-ts* mutations (Figure 6, A and B). Milder growth defects were also apparent when *COY1* was overexpressed in the *sec18-1* and *bet1-1* strains, while no phenotype was observed when *COY1* was overexpressed in strains bearing mutations in Golgi-associated tethering factors, including *grh1Δ*, *imh1Δ*, *rud3Δ, sgm1Δ, trs33Δ*, and *ypt1-3* (Supplemental Table 1). These genetic interactions implicate Coy1 in a functional network with the COG complex, Sed5, and Sly1.

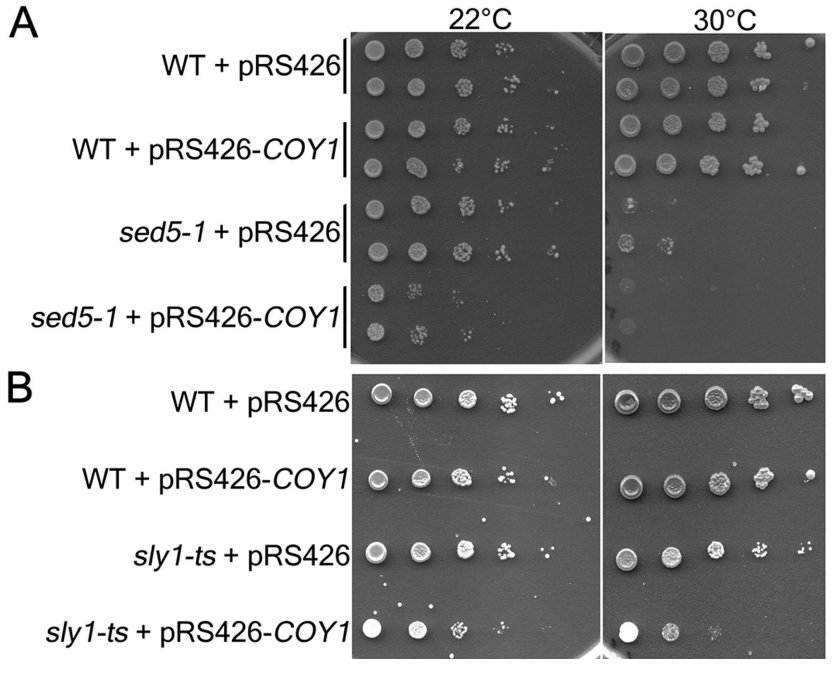


**FIGURE 6:** *COY1* genetically interacts with *sed5-1* and *sly1-ts*. (A) The *sed5-1* (CBY263) and isogenic wild-type strain (CBY267) were transformed with either an empty vector (pRS426) or a 2μ *COY1* overexpression vector (pRS426-*COY1*). Two independent isolates per transformations were serially diluted on selective media and grown at the indicated temperatures. (B) The *sly1-ts* strain (CBY268) and isogenic wild-type strain (CBY267) were transformed with either an empty vector or the *COY1* overexpression vector and subjected to growth assays as in A.

### Coy1 interacts with intra-Golgi retrograde tethering and fusion machinery

We next examined whether Coy1 could be detected in complex with any of the components suggested by genetic interactions. To this end, Coy1 was immunoprecipitated from digitonin-solubilized spheroplasts derived from wild-type cells with anti-Coy1 polyclonal antibodies. Coy1 was enriched in the immunoprecipitate, and Cog3, Sly1, and Gos1 were all pulled down with Coy1 antibodies (Figure 7A). These interactions were specific, as none of the coimmunoprecipitating proteins were detected in control reactions in which the preimmune serum was used.

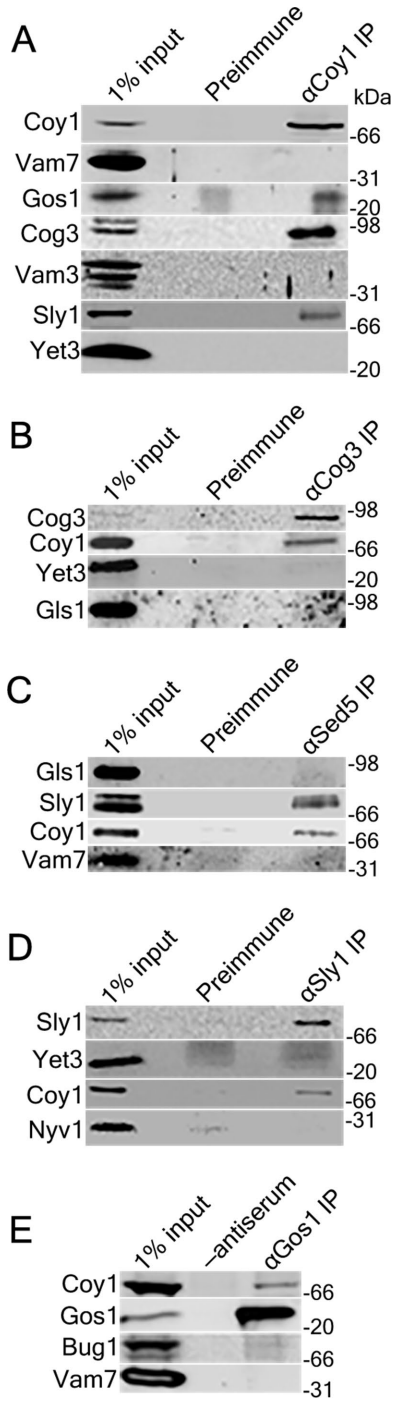


**FIGURE 7:** Coy1 interacts with Sly1, Cog3, Gos1, and Sed5. **(A)** Wild-type (CBY740) semi-intact membranes were solubilized with digitonin and immunoprecipitated (IP) with magnetic beads that had been preincubated with either Coy1 antiserum (αCoy1 IP) or preimmune serum from the same animal (Preimmune). Immunoprecipitates were washed, eluted in sample buffer, and resolved on 10.5% SDS–PAGE gels. Input represents a sample of the solubilized membranes prior to incubation with the antibody-bound beads. Immunoblotting was performed with polyclonal antiserum directed against Coy1, Sly1, Cog3, and Gos1, with the vacuolar SNAREs Vam3 and Vam7 and the ER resident protein Yet3 serving as negative controls. Positions of the MW ladder are indicated to the right of the blots. (B) Immunoprecipitation was conducted as described in A with antibodies directed against Cog3 or with preimmune serum. Blotting was conducted for Cog3 and Coy1, with Yet3 and Gls1 as negative controls. (C) Immunoprecipitation was conducted as described in A, using αSed5 preimmune and immune serum. Sed5 could not be detected in the immunoprecipitate, and its partner SM protein Sly1 served as a positive control instead. (D) Immunoprecipitation was conducted as described above with αSly1 antiserum or preimmune serum. Blotting was conducted against Sly1 and Coy1, with Yet3 and the vacuolar SNARE Nyv1 serving as negative controls. (E) Immunoprecipitates were prepared and processed as described above, using antiserum against Gos1. As Gos1 preimmune serum was not available, magnetic beads alone served as a negative control (-antiserum). Blotting was conducted for Gos1 and Coy1, with the golgin Bug1 and the vacuolar SNARE Vam7 functioning as negative controls.

Moreover, the ER resident protein Yet3 and the vacuolar SNAREs Vam3 and Vam7 were not detected in the immunoprecipitate, further supporting specificity. In reciprocal experiments, Coy1 could be coimmunoprecipitated with antibodies against Cog3 (Figure 7B), Sed5 (Figure 7C), Sly1 (Figure 7D), and Gos1 (Figure 7E). Thus Coy1 appears to exist in complex with Cog3, Sed5, Sly1, and Gos1.

We addressed whether Coy1 could directly interact with proteins that were recovered in coimmunoprecipitates through a series of in vitro binding assays. First, the cytosolic domains of a panel of soluble Golgi SNAREs were expressed and purified as glutathione *S*-transferase (GST) fusion proteins (Supplemental Figure 3A; Tsui and Banfield, 2000). Then yeast cells overexpressing Coy1ΔTM-HA were lysed and centrifuged at 120,000 × *g* to generate a Coy1-enriched high-speed supernatant fraction. The fusion proteins were then immobilized on glutathione agarose resin and incubated with this supernatant fraction. The resin was washed, bound proteins were eluted with sample buffer, and Coy1ΔTM-HA was detected by immunoblotting with a monoclonal αHA antibody. Coy1 was not appreciably pulled down by GST alone or by GST fusions to the ER-to-Golgi Qc-SNARE Bet1 or the retrograde Golgi R-SNARE Ykt6. In contrast, nearly 15% of the total Coy1ΔTM-HA added to the reaction could be recovered by GST-Gos1, GST-Sed5, and GST-Sft1 (Figure 8A). These results indicate that Coy1 specifically interacts with intra-Golgi retrograde Q-SNAREs.

To test whether Coy1 physically interacts with the COG complex, Lobe A of the COG complex, which consists of Cog1, Cog2, Cog3, and Cog4, was expressed and purified from bacteria as previously described (Supplemental Figure 3B; Lees *et al.*, 2010). Recombinant, purified COG was then immobilized on NiNTA resin and incubated with the Coy1ΔTM-HA enriched supernatant fraction. This fraction was also incubated with untreated NiNTA resin to measure background binding of Coy1ΔTM-HA. The resins were washed and eluted as described above. Less than 1% of the Coy1ΔTM-HA added to the reaction was recovered on the resin alone, whereas 20% of Coy1ΔTM-HA could be recovered with the COG complex bound to the resin (Figure 8B). Thus Coy1 physically interacts with the COG complex in vitro.

As the COG complex directly interacts with Sed5 (Suvorova *et al.*, 2002), we sought to test whether the interaction between Coy1ΔTM-HA and Sed5 was attributable to any residual COG complex in the cytosolic input used as a source of Coy1ΔTM-HA. We observed that Coy1 was readily resolved from the COG complex by gel filtration chromatography (Figure 8C). Coy1 eluted prior to Cog3 and another control protein, Sec13, when detergent-solubilized semi-intact wild-type cells were injected onto a Superose 6 column. A similar elution pattern was observed when cytosol from the Coy1ΔTM-HA (CBY3484) strain was gel filtered, although the Coy1 peak was shifted one fraction later, perhaps attributable to reduced protein abundance of Coy1ΔTM-HA relative to full length Coy1.

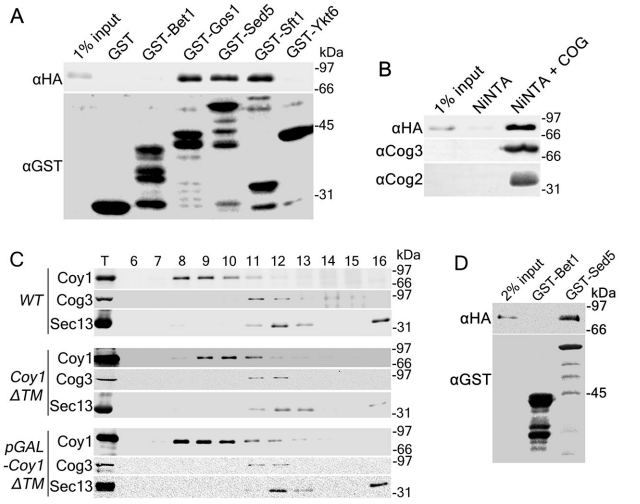


**FIGURE 8:** Coy1 directly interacts with multiple Golgi SNAREs and with lobe A of the COG complex. (A) Lysate from pGAL-Coy1ΔTM-HA (CBY3588) was diluted in binding buffer and centrifuged at 120,000 × *g* to generate a supernatant enriched in Coy1ΔTM-HA. This supernatant fraction was incubated with GST fusion proteins purified from *E. coli* and immobilized on glutathione-agarose resin. This resin was then washed, eluted with sample buffer, and resolved by SDS–PAGE. Immunoblotting was conducted using a monoclonal αHA antibody to monitor Coy1 recovery and with antiserum raised against GST-Yet3 to confirm the presence of each GST-tagged SNARE. Less than 1% of the total input is brought down by GST, GST-Bet1, or GST-Ykt6, while ~15% of Coy1ΔTM-HA is recovered by GST-Gos1, GST-Sed5, and GST-Sft1 (B) Supernatant fractions enriched in Coy1ΔTM-HA were prepared as in A and incubated with untreated NiNTA resin or purified COG1-4 (purified from *E. coli* and immobilized on NiNTA resin). Samples were incubated, washed, and eluted as in B. Immunoblotting was conducted with monoclonal antibodies against the HA epitope and with polyclonal antiserum against Cog3 and Cog2. Trace amounts of Coy1ΔTM-HA are brought down with the untreated resin (≤1%), while 20% of the input is recovered with the NiNTA-bound COG complex. (C) Top, Triton X-100 solubilized semi-intact cells from WT (CBY740) cultures were injected onto a Superose 6 column (GE Healthcare). Fractions were resolved on 10.5% SDS–PAGE gels and immunoblotted for Coy1, Cog3, and Sec13. Middle, Cytosol from Coy1ΔTM-HA (CBY3484) semi-intact cells diluted in binding buffer was injected onto a Superose 6 column and fractions were immunoblotted as above. Bottom, Cytosol from pGAL-Coy1ΔTM-HA cells was centrifuged and fractionated as described above. (D) Cytosol from pGAL-Coy1ΔTM-HA cells was resolved on a Superose 6 column. Fractions 8 and 9 were pooled and then aliquoted into tubes containing immobilized GST-Bet1 or GST-Sed5. Binding assays and immunoblotting were conducted as described in A.

Coy1ΔTM-HA was also resolved from Cog3 when cytosol from pGAL-Coy1ΔTM lysate was fractionated on the Superose 6 column. Coy1ΔTM-HA was efficiently captured by GST-Sed5 when the gel-filtered fractions depleted of the COG complex were used as the input for this binding reaction (Figure 8D). We conclude that the interaction between Coy1 and Sed5 is not mediated by the COG complex.

## DISCUSSION

Proper functioning of the Golgi complex requires compartmentalization of this organelle, yet many resident Golgi proteins are not restricted to one cisterna. Instead, these resident proteins dynamically cycle through the Golgi complex and are retrieved to earlier compartments by dedicated vesicular transport pathways. How these vesicles are targeted to and fused with specific cisterna remains an active area of investigation. In this report, we establish a role for the golgin protein Coy1 in intra-Golgi retrograde transport based on genetic and biochemical evidence. We find that the half-life of Och1, a resident Golgi protein known to undergo COPI- and COG-dependent retrograde transport (Harris and Waters, 1996; Spang and Schekman, 1998; Bruinsma *et al.*, 2004), is reduced in a *coy1Δ* strain (Figure 4), indicating a defect in the retrieval of this mannosyltransferase. We expect that this role in intra-Golgi retrograde transport is conserved, as microinjection of CASP, the human homologue of Coy1, inhibits retrograde transport of GalNAc-T2 without affecting retrograde transport of ERGIC53 in BSC-1 cells (Malsam *et al.*, 2005). Glycosylation defects were not apparent in *coy1Δ* or in cells lacking other golgins (Sgm1 and Rud3) putatively involved in tethering retrograde-directed COPI vesicles (Kim *et al.*, 1999; Kim, 2003; VanRheenen *et al.*, 1999; Fridmann-Sirkis *et al.*, 2004; Siniossoglou, 2005; Wong and Munro, 2014). However, cells lacking *SGM1* and either *COY1* or *RUD3* exhibited glycosylation and growth defects, and these phenotypes were further exacerbated in the triple knockout (Figure 5, A–C). These glycosylation defects are mechanistically attributable in part to disrupted membrane association of the COG complex, as the COG complex redistributes from the membrane to the cytosolic fraction in *coy1Δ* and *sgm1Δ* cells, and this shift is intensified in *coy1Δ sgm1Δ* double mutant cells (Figure 5, D and E). These results establish Coy1, Rud3, and Sgm1 as collectively important for the maintenance of glycosylation fidelity and reveal a shared role for the golgins in recruiting the COG complex to Golgi membranes.

These findings could be interpreted to indicate functional redundancy among Coy1, Rud3, and Sgm1, but several features set Coy1 apart from these other golgins. First, golgins are considered to share the same general topology: an N-terminus that extends into the cytoplasm and a C-terminus that is anchored to the Golgi (Witkos and Lowe, 2015; Gillingham and Murno, 2016). Small activated GTPases bind to the C-termini of Rud3 and Sgm1 to recruit them to the Golgi (Fridmann-Sirkis *et al.*, 2004; Gillingham *et al.*, 2004; Drin *et al.*, 2008). In contrast, the C-terminal transmembrane domain of Coy1 was not strictly required for its enrichment at the Golgi (Figure 3), suggesting that these general models of golgin topology may be oversimplified. The presence of Coy1ΔTM at the Golgi also indicates that the cytosolic region of Coy1 interacts with other proteins on this organelle. Indeed, we identified Coy1 in complex with the t-SNAREs Gos1 and Sed5, the early Golgi SM protein Sly1, and Cog3 via coimmunoprecipitation (Figure 7). In addition, Coy1ΔTM-3HA was efficiently captured by Sed5, Gos1, and Lobe A of the COG complex in vitro (Figure 8). The more diffuse sedimentation pattern of Coy1ΔTM-3HA in sucrose gradients (Figure 3C) can also be explained by these interactions, as many of the proteins Coy1 physically interacts with dynamically cycle between the Golgi and ER or the Golgi and endosomal system (Wooding and Pelham, 1998; Tai *et al.*, 2004). The transmembrane domain of Coy1 is not strictly required for enrichment of Coy1 at the Golgi, but it is functionally indispensable, as growth of *coy1Δ rud3Δ sgm1Δ* cells on calcofluor white is not rescued by a plasmid encoding Coy1ΔTM-3HA (Supplemental Figure 2B). Although the precise contribution of Coy1's transmembrane domain remains to be determined, the physical interactions Coy1 makes with Gos1, Sed5, and the COG complex suggest a role for Coy1 in bridging fusion and tethering machinery. This function further distinguishes Coy1 from other golgins, including

Rud3 and Sgm1, because most golgins are considered to primarily function as vesicle tethers (Kim *et al.*, 1999; VanRheenen *et al.*, 1999; Siniossoglou, 2005).

CASP was initially thought to function as a tether for retrograde directed Golgi vesicles, but this conclusion has come into dispute. CASP and golgin-84 were proposed to interact with one another on opposing membranes as a means of tethering retrograde directed vesicles to the Golgi, as these proteins coimmunoprecipitated with one another and golgin-84, but not CASP, was readily incorporated into COPI vesicles in an in vitro budding assay. Further support for this hypothesis was provided in vitro when CASP was demonstrated to capture vesicles laden with resident Golgi proteins, including golgin-84 (Malsam *et al.*, 2005). This result stands in contrast to a more recent report that demonstrated that mitochondrially anchored CASP is unable to redistribute any resident Golgi proteins to this ectopic site, including its proposed tethering partner, golgin-84 (Wong and Munro, 2014). How can these discrepancies be resolved? It is notable that CASP could only capture vesicles that had shed their COPI coat (Malsam *et al.*, 2005). Although it is not clear when the COPI coat is removed during intra-Golgi retrograde transport, there is a precedent for coat proteins serving as substrates for tethers (Cai *et al.*, 2007; Angers and Merz, 2009; Ren *et al.*, 2009; Zink *et al.*, 2009). Underscoring this possibility, the COG complex and the COPI coat copurify with one another, and COPI-coated vesicles accumulate in the cytoplasm of HeLa cells upon knockdown of *COG3* (Suvorova *et al.*, 2002; Zolov and Lupashin, 2005). Therefore we propose that retrograde-directed COPI-coated vesicles are first captured by other golgins, either alone or in combination with the COG complex (Wong and Munro, 2014; Willet *et al.*, 2013). Once tethered, removal of the coat could permit transfer of the vesicle to CASP. What might CASP bind that is only accessible after uncoating? The vesicular SNARE GS15 represents a promising candidate, as our in vitro binding assays establish a direct interaction between Coy1 and Sft1, the yeast homologue of GS15 (Figure 8B). As Coy1 also physically interacts with Sed5 and Gos1 (Figures 7, A, C, and E, and 8B), an exciting implication of these findings is that Coy1 could serve to distally connect the v-SNARE to a cognate set of t-SNAREs. Our results offer a potential means of reconciling seemingly contradictory results.

These physical interactions also contextualize the genetic interactions exhibited by *COY1*. Overexpression of *COY1* is toxic in *gos1Δ* (Gillingham *et al.*, 2002), *sed5-1*, and *sly1-ts* cells (Figure 6), while the deletion of *COY1* suppresses the growth defect and partially suppresses the temperature sensitivity of *cog3-2* without rescuing this strain's glycosylation and transport defects (Figure 5, F and G). As Coy1 has no direct role in anterograde transport (Figure 1B), we speculate that Coy1 binds Sed5 to reserve this syntaxin for use in intra-Golgi retrograde transport, perhaps by enhancing interactions between Sed5 and either Gos1 or the COG complex (Suvorova *et al.*, 2002; Shestakova *et al.*, 2007). By sequestering Sed5 for use in retrograde transport, Coy1 would also indirectly diminish the incorporation of Sed5 into the anterograde SNAREpin (Tsui *et al.*, 2001; Parlati *et al.*, 2002). Consistent with this assumption, a mild anterograde transport defect is observed in a strain overexpressing *COY1* (Supplemental Figure 1), while microinjection of soluble CASP into BSC-1 cells also modestly slows anterograde transport of VSV-G (Malsam *et al.*, 2005). If retrograde transport is dysfunctional (as in *gos1Δ* or *cog3-2)* or if components required for both anterograde and retrograde transport pathways at the early Golgi have been compromised (*sed5-1* or *sly1-ts*), then this proposed function of Coy1 would prove deleterious, as Sed5 would be restricted to a transport process that is either inefficient or less essential, respectively (Liu *et al.*, 2015; Papanikou *et al.*, 2015). Removing Coy1 from this context would dysregulate transport through the Golgi (consistent with elevated CPY secretion in *cog3-2 coy1Δ*) while freeing up Sed5 for use in anterograde trafficking. As secretory protein transport and biosynthesis are coordinated with one another (Lipschutz *et al.*, 2003; Toikkanen *et al.*, 2003; Cancino *et al.*, 2014; Luini *et al.*, 2014), we speculate that the loss of *COY1* restores viability to *cog3-2* cells by enhancing the delivery of nascent proteins to the Golgi, obviating the need for a robust recycling pathway.

The suppression of the growth defects and temperature sensitivity of *cog3-2* by *coy1Δ* appears to parallel the rescue of the *grh1Δ* tethering defect by *coy1Δ*. Both the COG complex and Grh1 were initially proposed to function in anterograde transport because anterograde transport efficiency is diminished when the functionality of these proteins is absent (VanRheenen *et al.*, 1998, 1999; Behnia *et al.*, 2007). The detrimental effect on ER-to-Golgi transport for COG mutants has since been explained as an indirect consequence of disrupted retrograde Golgi transport (Ballew *et al.*, 2005). Similarly, a direct role for Grh1 in tethering COPII vesicles has been contested based on the absence of an effect on vesicle accumulation between the tER and Golgi in a *grh1Δ* strain of *Pichia pastoris* (Levi *et al.*, 2010). As knockdown of the mammalian homologues of *GRH1* or *COG3* results in fragmentation of the Golgi, disrupted anterograde transport in *grh1Δ*, *cog3-2*, and *cog2-1* could arise as an indirect consequence of aberrant Golgi morphology rather than a loss of factors directly required for COPII vesicle capture (Zolov and Lupashin, 2005; Puthenveedu *et al.*, 2006). As our data implicate Coy1 in regulating Golgi SNARE availability and function, we speculate that the loss of Coy1 would suppress Golgi fragmentation by increasing the promiscuity of vesicle consumption at the Golgi or enhancing the rate of homotypic cisternal fusion (Bhave *et al.*, 2014).

Although much remains to be determined on how Coy1 affects the function of COG complex and SNAREs, our present work establishes a role for this golgin at the interface between vesicle tethering and fusion. As our understanding of how tethering proceeds to fusion remains limited at present, Coy1 represents an exciting case study on how these processes may be coordinated with one another. To this end, it will be essential to determine which regions of Coy1 are required to interact with the COG complex and SNARE proteins and if Coy1 can interact with COG subunits and one or more SNAREs simultaneously. Integrating genetic and phenotypic analyses with in vitro reconstitution experiments should further elucidate our understanding of Coy1 and its role in intra-Golgi retrograde transport.

## MATERIALS AND METHODS

### Yeast strains and media

Yeast strains used in this study are listed in Table 1. Unless otherwise noted, strains were cultured on YPD (1% bacto-yeast extract, 2% bacto-peptone, 2% glucose [Becton, Dickson, and Company, Franklin Lakes, NJ]) or YMD for auxotrophic selection (0.7% yeast nitrogen base without amino acids, 2% glucose, and Complete Supplement Mixture [MP Biomedicals, Solon, OH]). Strain growth was monitored by absorbance at 600 nm ($OD_{600}$) on a GeneSys 10S UV-Vis spectrophotometer (Thermo Fisher, Waltham, MA).

### Strain and plasmid construction

The lithium acetate method was used for yeast transformation (Ito *et al.*, 1983). The pRS426-*COY1* plasmid was previously described (Gillingham *et al.*, 2002). To generate Coy1-HA (CBY2674), CBY740

| Strain | Genotype | Reference |
|---|---|---|
| RSY248 | *MATα his4-619* | Kaiser and Schekman (1990) |
| RSY263 | MATα sec12-4 ura3-52 | Kaiser and Schekman (1990) |
| RSY944 | *MATa ura3-52 lys2-801 bet1-1* | Cao *et al.* (1998) |
| CBY263 | *MATα trp1-1 ade2-1 ura3-1 leu2-3,112 can1-100 sed5-1* | Cao *et al.* (1998) |
| CBY267 | *MATα trp1-1 ade2-1 ura3-1 leu2-3,112 can1-100* | Mizuta and Warner (1994) |
| CBY268 | *MATα trp1-1 ade2-1 ura3-1 leu2-3,112 can1-100 sly1-ts* | Mizuta and Warner (1994) |
| CBY474 | *MATα trp1-1 ade2-1 ura3-1 leu2-3,112 can1-100 ypt1-3* | Cao *et al.* (1998) |
| CBY740 = BY4742 | *MATα his3Δ1 leu2Δ0 lys2Δ0 ura3Δ0* | Brachmann *et al.* (1998) |
| CBY742 = BY4741 | *MATa his3Δ1 leu2Δ0 met15Δ0 ura3Δ0* | Brachmann *et al.* (1998) |
| CBY1702 | CBY740 with *sec18-1* | Heidtman *et al.* (2003) |
| CBY2009 | CBY740 with *grh1Δ::kanMX6* | Research Genetics |
| CBY2030 | CBY740 with *imh1Δ::kanMX6* | Research Genetics |
| CBY2289 | CBY740 with *trs33Δ::kanMX6* | Research Genetics |
| CBY2659 | CBY742 with *coy1Δ::kanMX6* | Research Genetics |
| CBY2660 | *CBY740* with *coy1Δ::kanMX6* | Research Genetics |
| CBY2666 | CBY740 with *cog6Δ::kanMX6* | Research Genetics |
| CBY2674 | *CBY740 with COY1::3HA-HIS3MX6* | This study |
| CBY2678 | CBY740 with *rud3Δ::kanMX6* | Research Genetics |
| CBY2692 | CBY2660 with *rud3Δ::kanMX6* | This study |
| CBY3178 | CBY2009 except *grh1Δ::natMX4* | Research Genetics |
| CBY3258 | CBY3178 with *coy1Δ::kanMX6* | This study |
| CBY3481 | CBY740 with pGAL-COY1::kanMX6 | This study |
| CBY3484 | CBY3481 with *COY1(1-613)::3HA-HIS3MX6* | This study |
| CBY3588 | CBY3484 with *kanMX6-pGAL::COY1ΔTM-3xHA* | This study |
| CBY3874 | CBY740 with *sgm1Δ::kanMX6* | Research Genetics |
| CBY3881 | CBY740 with *cog3Δ::*cog3-2*natMX6* | This study |
| CBY4101 | CBY2678 *with sgm1Δ::hphMX6* | This study |
| CBY4102 | CBY2660 *with sgm1Δ::hphMX6* | This study |
| CBY4103 | CBY4101 with *coy1Δ::natMX6* | This study |
| CBY4788 | CBY3881 with *coy1Δ::kanMX6* | This study |

**TABLE 1:** Yeast strains used in this study.

was transformed with PCR product generated from pFA6a-3HA-His3MX6 that was targeted to fuse in frame after the last codon of *COY1* (Longtine *et al.*, 1998). The *coy1Δ rud3Δ* strain (CBY2692) was generated by mating CBY2659 (a *coy1Δ*) and CBY2678 (α rud3*Δ*). Haploids generated from this mating were screened by colony PCR to confirm disruption of both genes. The *grh1Δ::nat* strain (CBY3178) was generated by transforming *grh1Δ::kan* (CBY2009) with the nourseothricin-resistance gene from p4339 and selecting isolates that were resistant to nourseothricin and sensitive to geneticin (Tong *et al.*, 2001). The *coy1Δ grh1Δ* strain (CBY3258) was produced by mating CBY2659 (a *coy1Δ::kan)* with CBY3178 (α *grh1Δ::nat)* and selecting haploids that were resistant to both nourseothricin and geneticin. A strain expressing Coy1ΔTM-HA (CBY3484) was constructed in CBY740 using pFA6a-3HA-His3MX6 to generate an in-frame fusion immediately after amino acid residue 613 of Coy1. To generate CBY3481, the pFA6a-kanMX6-pGAL cassette was directed to replace the endogenous *COY1* promoter with the *GAL1* promoter in a wild type (CBY740). A strain expressing Coy1ΔTM-HA under the *GAL1* promoter was constructed by transforming CBY3481 with the pFA6a-3HA-His3MX6 cassette to truncate *COY1* after the region encoding amino acid 613 (Longtine *et al.*, 1998). The *cog3-2* mutant allele in the CBY740 background (CBY3881) was constructed using established methods (Tong and Boone, 2006; Wilson and Barlowe, 2010). First, the *cog3-2* ORF plus 179 downstream base pairs was amplified using genomic DNA isolated from CBY559 (VanRheenen *et al.*, 1999). The nourseothricin resistance gene was then amplified from pFA6a-natMX6 using primers designed to fuse this cassette immediately downstream of the amplified *cog3-2* ORF (Hentges et al, 2005). These constructs were then transformed into CBY740. Isolates were screened for nourseothricin resistance, temperature sensitivity, and truncation of the 98-kDa Cog3 protein via immunoblotting (Wuestehube *et al.*, 1996; VanRheenen *et al.*, 1998; Kim *et al.*, 1999). The *SGM1* gene was disrupted in the *rud3Δ* (CBY2678) and *coy1Δ* (CBY2660) backgrounds using the Hygromycin B resistance gene from the plasmid pFA6a-hphMX6,

yielding *rud3Δ* sgm1*Δ* (CBY4101) and *coy1Δ sgm1Δ* (CBY4102). *COY1* was then disrupted in the *rud3Δ sgm1Δ* (CBY4101) strain with the nourseothricin resistance gene using pFA6a-natMX6 plasmid (Hentges *et al.*, 2005). The *cog3-2 coy1Δ* strain (CBY4788) was constructed by mating *coy1Δ* (CBY2659) with *cog3-2* (CBY3881). Spores from this cross were plated on YPD + geneticin + nourseothricin. Antibiotic-resistant haploid cells were screened by immunoblotting with anti-Cog3 and anti-Coy1 antibodies to confirm the mutant alleles.

The pRS426 Coy1ΔTM plasmid was constructed by amplifying the *PHO5* promoter region through the first 1842 base pairs of the *COY1* ORF from the pRS426 *COY1* plasmid (Gillingham *et al.*, 2002) with a *Xho*I restriction site encoded on the forward primer (GTAATTATAACTCGAGGTCGACGCTCTCCCTT) and a pair of stop codons followed by a *Sac*I restriction site on the reverse primer (GAAAATGTTTGAGCTCTTATTACCTTGTCATTTTATTTTGTAAAATGACTTTTGCAAAAC). The amplified fragment and the pRS426 plasmid were digested with *Xho*I and *Sac*I-HF restriction enzymes and ligated together. Ligation reactions were transformed into DH5α, and the sequence of the plasmid was verified by Sanger sequencing. Expression of Coy1ΔTM from this plasmid was verified by immunoblotting lysates derived from a *coy1Δ* (CBY2660) strain transformed with this plasmid with the polyclonal Coy1 antibody.

### Antibodies and immunoblotting

Polyclonal antibodies have been previously described for CPY (Rothblatt *et al.* 1989), Gas1 (Fankhauser and Conzelmann 1991), Sec63 (Feldheim *et al.*, 1992), Kar2 (Brodsky and Schekman 1993), Sec13 (Salama *et al.*, 1993), Erv25 (Belden and Barlowe 1996), Sec19 (Barlowe 1997), Sly1 and Sed5 (Cao *et al.* 1998), Vam3 (Ungermann *et al.* 1998), Och1 and Erv41, Erv46 (Otte *et al.*, 2001), Vam7 (Merz and Wickner 2004), Nyv1 (Thorngrenn *et al.* 2004), Cog2 and Cog3 (Ballew *et al.* 2005), Gos1 (Inadome *et al.* 2005), Yet3 (Wilson and Barlowe 2010), and Gls1 (Shibuya *et al.* 2015). Monoclonal antibodies against the HA epitope (HA.11) were purchased from BioLegend (San Diego, CA). Primary antibodies were used at a 1:1000 dilution. Horseradish peroxidase–conjugated donkey anti-rabbit and sheep anti-mouse secondary antibodies were utilized for detection of the polyclonal and monoclonal antibodies, respectively, at a dilution of 1:10,000 (GE Healthcare, Chicago, IL). Supersignal West Pico Chemiluminescent substrate (Thermo Fisher, Waltham, MA) and a G:BOX Chemi XR5 (Syngene, Frederick, MD) were used to detect chemiluminescence. Immunoblot signal intensity was quantified by densitometric analysis using the Syngene GeneTools analysis software.

Polyclonal anti-Coy1 antiserum was raised against a glutathione *S*-transferase (GST) fusion protein, GST-Coy1, containing amino acid residues 1–613 of Coy1. The GST-Coy1 fusion was expressed as a 100-kDa protein in *Escherichia coli* BL21 cells and was contained in inclusion bodies that fractionated in the 15,000 rpm pellet of cell lysates. Inclusion body pellets were washed with Tris-buffered saline (TBS) containing 1.0% Triton X-100 and then washed and resuspended in TBS. The resuspended pellet was used as antigen in rabbits (Covance, Denver, PA).

To generate polyclonal antiserum against Bug1, full-length Bug1 was purified from *E. coli* by Intein Mediated Purification using the Affinity Chitin-binding Tag system from New England Biolabs (Ipswich, MA). Bug1 was cleaved from its affinity tag after purification and used as an antigen in rabbits (Covance, Denver, PA).

### Membrane preparations and subcellular fractionation

Strains were converted to spheroplasts as previously described (Baker *et al.*, 1988). Sucrose gradient centrifugation experiments were conducted as described by Powers and Barlowe with minor modifications (1998). Spheroplasts were resuspended in 10 mM HEPES, pH 7.4, 1 mM EDTA, 12.5% sucrose, and 1 mM phenylmethylsulfonyl fluoride (PMSF) and lysed by 10 strokes of a chilled Potter-Elvehjem homogenizer. The lysate was centrifuged for 4 min at 3500 rpm at 4°C in an SS-34 rotor, after which the supernatant was recovered and layered atop a t10-step sucrose gradient (from 54–18% on top of a 2-ml 60% sucrose cushion in 10 mM HEPES, pH 7.4, 1 mM $MgCl_2$). Gradients were centrifuged in an SW-40 rotor at 36,000 rpm for 3 h at 4°C, and 785-µl fractions were collected from the top to the bottom of the gradient. Samples from each fraction were diluted with an equal volume of sample buffer, boiled at 75°C for 10 min, resolved on 10.5% SDS–PAGE gels, and immunoblotted using polyclonal antibodies against Coy1, Gls1 (as an ER and vacuolar marker), Erv25 (Golgi and ER marker), Och1 (Golgi marker), and CPY (vacuole marker).

ER- and Golgi-enriched membrane pellets were prepared following an ER export block as previously described with modifications (Heidtmann *et al.*, 2003, Mukherjee and Barlowe, 2016). Wild-type (RSY248) and *sec12-4* strains (RSY263) were grown overnight at room temperature, back-diluted to an $OD_{600}$ of 0.1, and grown to mid log phase at 25°C. Cycloheximide was added to 50 µg/ml to minimize protein translation (Todorow *et al.*, 2000). Cell cultures were incubated for 20 min at 25°C and then transferred to a 38.5°C water bath for 90 min. Cells were harvested by centrifugation and converted to spheroplasts. The spheroplasts were resuspended in 2.5 ml JR lysis buffer (20 mM HEPES, pH 7.4, 0.1 M sorbitol, 50 mM potassium acetate (KOAc), 2 mM EDTA, 1 mM PMSF, and 1 mM dithiothreitol [DTT]), homogenized with six strokes of a Potter–Elvehjem homogenizer, and centrifuged at in a SS-34 rotor at 4000 rpm at 4°C for 5 min to pellet nuclei and unbroken cells. The supernatant was recovered and centrifuged at 14,000 rpm for 10 min at 4°C (Eppendorf 5417R) to generate the ER-enriched p13 pellet. The supernatant from this spin was recovered and centrifuged at 60,000 rpm for 15 min at 4°C in a TLA 100.3 rotor, yielding a Golgi-enriched p100 pellet. The p13 and p100 pellets were resuspended in 100 µl JR lysis buffer, diluted 1:1 with 5× sample buffer, boiled, and separated on 10.5% SDS–PAGE gels. Immunoblotting was conducted with polyclonal antibodies against Coy1, Erv41, and Erv46.

For COG membrane association assays, yeast semi-intact cells from wild type (CBY740), *coy1Δ* (CBY2660), *sgm1Δ* (CBY3874), and *coy1Δ sgm1Δ* (CBY4102) cultures were diluted in 20 mM HEPES, pH 6.8, 250 mM sorbitol, 150 mM KOAc, 5 mM $Mg(OAc)_2$ (B88) + 1 mM PMSF + 5 mM EDTA + 1 mM DTT to a final concentration of 6 $A_{280}$ units/ml. Samples were centrifuged at 54,000 rpm for 20 min in a TLA 100.3 rotor. Samples of the supernatant fractions were diluted in sample buffer and the remaining supernatant was aspirated off. After resuspending the pellet in B88, an equivalent volume of the pellet was diluted into sample buffer, and the fractions were resolved on 10.5% SDS–PAGE gels. Immunoblotting was conducted with antiserum against Cog3, Sec19, Och1, and Yet3. Statistical analyses were performed with GraphPad Prism 7 software.

### In vitro vesicle budding, tethering, and transport assays

Analytical scale COPII budding assays were performed as previously described (Barlowe *et al.*, 1994) using washed microsomes derived from wild-type cells (Wuestehube and Schekman, 1992). Tethering and fusion assays were performed as described by Cao *et al.* (1998). The average of duplicate measurements is shown in Figure 1, B–D, with the error bars representing the range.

### Indirect immunofluorescence microscopy

The localization of Coy1-HA and Coy1ΔTM-HA was monitored by immunofluorescence microscopy as described by Powers and Barlowe (1998). Cells were fixed with formaldehyde, converted to spheroplasts, and adhered to slides coated with polylysine. Cells were washed, incubated at room temperature in blocking buffer (1% BSA and 0.5% Triton X-100 in phosphate-buffered saline [PBS]), and then incubated with primary antibodies. The anti-HA monoclonal antibody (HA.11) and the anti-Och1 antibody were both used at a dilution of 1:200, while the Kar2 antibody was used at a dilution of 1:300. Secondary Alexa Fluor 488 conjugated anti-mouse antibodies and Alexa Fluor 594 conjugated anti-rabbit antibodies were used at a dilution of 1:1000 (Thermo Fisher, Waltham, MA). Images were obtained at room temperature using a DeltaVision Imaging System (GE Healthcare, Chicago, IL), comprising a customized inverted wide-field microscope (IX-71; Olympus, Central Valley, PA), an UPlanS Apochromat 100×/1.40 NA lens (Olympus) with DeltaVision immersion oil ($n = 1.516$; GE Healthcare), a camera (CoolSNAP HQ2; Photometrics, Tucson, AZ), and an Insight solid-state illumination unit. Images were deconvoluted in SoftWoRx (GE Healthcare) and prepared with ImageJ (National Institutes of Health, Bethesda, MD) and Photoshop (Adobe, San Jose, CA).

### In vivo labeling

The pulse-chase experiments were performed as previously described (Belden and Barlowe 1996; Bue *et al.*, 2006). Wild-type (CBY740) or coy1Δ (CBY2660) cells were cultured at 30°C in YMD with reduced sulfate to an OD of 0.5, harvested, then washed and resuspended in YMD without sulfate to an $OD_{600}$ of 5. Cultures were incubated for 5 min in a 30°C water bath and then pulsed with [$^{35}$S] Promix (GE Healthcare, Chicago, IL) at a concentration of 8.3 µCi/$OD_{600}$ cells for 6 min. The chase was initiated by addition of excess unlabeled methionine and cysteine. After 0, 5, 10, 20, and 40 min, 1-ml samples of cells were taken and diluted into 4 ml ice-cold 20 mM $NaN_3$. Cells were then harvested by centrifugation, washed, and resuspended in 225 µl cold $NaN_3$ and then diluted with 225 µl 2× lysis buffer (100 mM Tris, pH 7.4, 2% SDS, 10 mM EDTA, 2 mM PMSF). Ice-cold glass beads were then added to the resuspended cells. Lysis was performed by vortexing the samples for 2 min, incubating at 95°C for 2 min, allowing the samples to cool to room temperature, vortexing for 5 min, and boiling again at 95°C for 1 min. After clearing the lysed samples by centrifugation at 14,000 rpm (Eppendorf 5415 C) for 1 min, 100-µl samples of lysate were diluted with 1 ml IP-SDS buffer (15 mM Tris, pH 7.5, 150 mM NaCl, 1% Triton X-100) and incubated overnight with 40 µl of a 20% Protein A sepharose slurry (GE Healthcare) and either 0.5 µl anti-Och1 or 1 µl anti-Kar2 antiserum. The resin was then washed twice with 1 ml IP-SDS buffer and eluted by boiling in sample buffer. Immunoprecipitates were resolved on 10.5% polyacrylamide gels and visualized by autoradiography using a phosphor screen on a Typhoon 8600 Variable Mode Imager and, later, on film. Half-lives were quantified using the ImageQuant 5.2 software (GE Healthcare).

### Immunoprecipitations

Immunoprecipitations were conducted as described by Bue and Barlowe (2009) with minor modifications. A 5% digitonin stock was prepared by adding 50 mg digitonin (EMD Millipore, Billerica, MA) to 1 ml sterile water, which was then boiled at 95°C for 10 min and allowed to cool at room temperature. Twenty microliters of Pierce Protein A magnetic beads (Thermo Fisher, Waltham, MA) was washed twice in B88-8 (20 mM HEPES, pH 8.0, 250 mM sorbitol, 150 mM KOAc, 5 mM $Mg(OAc)_2$) + 0.05% digitonin, resuspended to 1 ml, and incubated for 45 min with 1 µl of antibody. Beads were washed twice in B88-8 + 0.05% digitonin and set aside until the soluble extract had been prepared. Aliquots of wild-type spheroplasts (at 7.5 $A_{280}$ units per aliquot) were thawed, resuspended in 1 ml B88, and centrifuged once at 10,000 rpm for 2 min at 4°C to wash (Eppendorf 5417R). The supernatant was aspirated and the pellet was resuspended to 220 µl in B88-8 + 1 mM PMSF + 5 mM EDTA. The samples were incubated for 2 min in a 24°C water bath, after which 220 µl solubilization buffer was added (B88-8 + 1 mM PMSF + 5 mM EDTA + 2% digitonin). Samples were returned to the 24°C water bath, incubated for 15 min and centrifuged at 10,000 rpm for 2 min at room temperature (Eppendorf 5424). A sample of this supernatant was diluted in sample buffer as a means of monitoring the reaction input. The remaining supernatant was transferred to a fresh, chilled Eppendorf tube and diluted with 700 µl B88-8 + 1 mM PMSF + 5 mM EDTA + 0.5% digitonin. Washed, antibody-bound magnetic beads were added to the diluted samples and incubated for 2 h for the αCoy1 IP, or for 16 h for the reciprocal IPs. The reactions were then applied to a magnet, washed three times with B88-8 + 0.05% digitonin, and eluted by boiling in 30 ul sample buffer. Samples were separated on 10.5% polyacrylamide gels, and immunoblotting was conducted using polyclonal antibodies.

### Protein purification, binding assays, and gel filtration chromatography

GST fusion proteins were purified as described with some modifications (Parlati *et al.*, 2000; Tsui and Banfield, 2000; Peng and Gallwitz, 2002). Each plasmid (including pGEX-2T, pGST-BET1, pGST-GOS1, pGST-SED5, pGST-SFT1Δ11, pGST-YKT6, and pQLinkH COG1-4) was transformed into *E. coli* strain C43 DE3 for expression (Tsui and Banfield, 2000; Lees *et al.*, 2010). For the GST fusion proteins, starter cultures were back diluted 1:100 into 1 l lysogeny broth (LB) (1% tryptone, 0.5% yeast extract, 0.5% NaCl) with 50 µg/ml ampicillin. For GST, GST-Bet1, GST-Gos1, GST-Sft1, and GST-Ykt6, expression was induced with 0.5 mM IPTG at an $OD_{600}$ of 0.6 for 4 h. Cells were harvested by centrifugation at 3500 rpm for 15 min at 4°C in a F10B-6 × 500 rotor. Pellets were washed with 50 ml lysis buffer (25 mM HEPES, pH 7.5, 150 mM KOAc, 0.05% Tween-20) and resuspended in 40 ml lysis buffer + 5 mM DTT + 1 mM EDTA + one Complete protease inhibitor tablet (Roche, Indianapolis, IN). The GST-Sed5 culture was grown to an $OD_{600}$ of 0.6 and then induced with 0.5 mM isopropyl-β-D-thiogalactoside (IPTG) and shifted to 16°C for 18 h. GST-Sed5 was washed and lysed in a buffer composed of 25 mM HEPES, pH 7.5, 400 mM KCl, 10% glycerol, 1% Triton X-100, 5 mM DTT + 1 mM EDTA + 1 Complete protease inhibitor tablet. Cells were lysed by French press, and lysates were centrifuged at 14,000 rpm for 15 min at 4°C in a Sorvall SS34 rotor. Supernatants were incubated for 2 h at 4°C with 0.1 g preswollen glutathione-agarose resin (Sigma-Aldrich, Waldrich, MA). Unbound material was discarded and the resin was washed with 50 ml lysis buffer. Bound proteins were eluted in 10 ml lysis buffer with 10 mM glutathione. Proteins were further purified by anion exchange (Mono Q HR 5/5; GE Healthcare, Chicago, IL) and gel filtration (Superose 12 HR 10/30; GE Healthcare). Aliquots were then prepared, each corresponding to 50 µg of purified protein.

To purify lobe A of COG (Cog1-4), the same methodologies described by Lees *et al.* (2010) and Ha *et al.* (2016) were employed, with minor modifications. Cultures of *E. coli* C43(DE3) bearing pQLink COG1-4 were grown overnight at ambient temperature in LB and then back diluted 1:100 into 1 l terrific broth (1.2% tryptone, 2.4% yeast extract, 0.4% glycerol, 17 mM $KH_2PO_4$, and 72 mM

$K_2HPO_4$) with 100 µg/ml ampicillin. This culture was grown at 37°C to an $OD_{600}$ of 0.4, at which point it was shifted to a 22°C incubator and grown to an OD of 0.7. Cultures were then induced with 0.5 mM IPTG and incubated for 18 h. Cells were harvested by centrifugation and then washed and lysed by French press in COG lysis buffer (20 mM Tris, pH 8.0, 150 mM NaCl, 20 mM imidazole, 10 mM β-mercaptoethanol). Lysates were centrifuged at 45,000 rpm for 30 min at 4°C in a 60Ti fixed-angle rotor. The clarified supernatant was incubated for 90 min with 3ml NiNTA agarose (Qiagen, Hilden, GE) that had been equilibrated in COG lysis buffer. The lysate and resin was then applied to an Econo-Column (BioRad, Hercules, CA) to separate unbound material from the resin. The resin was then washed with 100 ml COG lysis buffer, and bound material was eluted with 10 ml COG lysis buffer + 500 mM imidazole. The eluate was applied to an anion exchange column (MonoQ HR 5/5) that had been equilibrated in 25 mM NaCl, 20 mM Tris, pH 8.0, and 10 mM β-mercaptoethanol and fractionated on a linear gradient rising to 1 M NaCl. COG-containing fractions were pooled, concentrated on a 30-kDa NMWCO Amicon 15 centrifugal ultrafiltration device (EMD Millipore, Billerica, MD), and injected onto a gel filtration column (Superose 6 HR 10/30, GE Healthcare) equilibrated with 20 mM Tris, pH 8.0, 150 mM NaCl, and 10 mM β-mercaptoethanol. Aliquots corresponding to 15 µg of purified COG were prepared and stored at -70°C.

To generate a Coy1-enriched yeast lysate, the *GAL1*-regulated Coy1ΔTM-HA strain (CBY3588) was grown overnight in 50 ml of YP + 1% galactose + 1% glucose. 100 $OD_{600}$ units from this culture were recovered, washed once with YP, and added to 1 l YP + 2% galactose + 0.1% glucose. The culture was harvested at late log phase ($OD_{600}$ = 2), washed with B88, and lysed with liquid nitrogen in a blender. Aliquots corresponding to 50 mg of the culture wet weight were then prepared and stored at -70°C.

For binding assays, aliquots of either the purified GST fusion proteins or of the COG complex were thawed, diluted with binding buffer (150 mM KOAC, 25 mM HEPES, pH 7.5, 250 mM sorbitol, 0.01% Triton X-100), and immobilized on glutathione agarose or NiNTA resin. Meanwhile, aliquots of the Coy1ΔTM-HA enriched lysate were thawed, diluted in Coy1 binding buffer + 1 mM PMSF + 1 mM DTT (and 20 mM imidazole, for the COG binding assay), and centrifuged at 55,000 rpm (TLA 100.3). Five hundred microliters of the high-speed supernatant (corresponding to ~ 15 mg culture wet weight) was added to each sample of immobilized protein, and reactions were incubated together for 3 h at 4°C while undergoing gentle rotation. The reactions were centrifuged at 14,000 rpm for 1 min at 4°C, and the unbound material removed. The beads were washed once with 500 µl Coy1 binding buffer, and bound proteins were eluted with 45 µl 5× sample buffer. Samples were analyzed on 9% or 10.5% polyacrylamide gels.

All gel filtration experiments were conducted with a Superose 6 10/300 column (GE Healthcare) at a flow rate of 0.3 ml/min and equilibrated in column buffer (150 mM KOAc, 250 mM sorbitol, 25 mM HEPES, pH 7.4, 0.1% Triton X-100). To fractionate endogenous Coy1, semi-intact cells from a wild-type strain (CBY740) were solubilized in column buffer with 1% Triton X-100 and 1 mM PMSF for 20 min on ice. Samples were centrifuged for 20 min at 14,000 rpm in a F-45-30-11 rotor in a chilled Eppendorf 5417r centrifuge, and 500 µl of the soluble extract was injected onto the Superose 6 column. Fractionation of Coy1ΔTM-HA (CBY3484) was conducted as above, except that the semi-intact cells were resuspended in column buffer with PMSF and without any additional Triton X-100 and centrifuged immediately afterward to minimize membrane solubilization. Aliquots from the liquid nitrogen lysate of pGAL-Coy1ΔTM-HA cells (CBY3588) were pooled, treated with 1 mM PMSF, and centrifuged and injected onto the column as described above. Fractions 8 and 9 of the pGAL-Coy1ΔTM-HA fractionation were pooled and aliquoted into tubes containing immobilized GST-Bet1 or GST-Sed5, and binding assays proceeded as described above with the exception that the resin was washed with column buffer rather than with binding buffer. All samples from the gel filtration and binding assays were analyzed on 10.5% SDS–PAGE gels.

## ACKNOWLEDGMENTS

We thank Sean Munro for providing the pRS426-COY1 plasmid and David Banfield for providing the plasmids for GST-SNARE protein expression. We also thank Fred Hughson for sending the pQLink COG1-4 vector for expression of COG complex. We thank Bill Wickner for providing antibodies against the vacuolar SNARE proteins Nyv1, Vam3, and Vam7. This work was support by National Institutes of Health grant GM-052549.

## REFERENCES

Albuquerque CP, Smolka MB, Payne SH, Bafna V, Eng J, Zhou H (2008). A multidimensional chromatography technology for in-depth phosphoproteome analysis. Mol Cell Proteomics 7, 1389–1396.

Angers CG, Merz AJ (2009). HOPS interacts with Apl5 at the vacuole membrane and is required for consumption of AP-3 transport vesicles. Mol Biol Cell 20, 4563–4574.

Baker D, Hicke L, Rexach M, Schleyer M, Schekman R (1988). Reconstitution of SEC gene product-dependent intercompartmental protein transport. Cell 54, 335–344.

Ballew N, Liu Y, Barlowe C (2005). A Rab requirement is not bypassed in SLY1-20 suppression. Mol Biol Cell 16, 1839–1849.

Banfield DK (2011). Mechanisms of protein retention in the Golgi. Cold Spring Harb Perspect Biol 3, a005264.

Barlowe C, Orci L, Yeung T, Hosobuchi M, Hamamoto S, Salama N, Rexach MF, Ravazzola M, Amherdt M, Schekman R (1994). COPII: a membrane coat formed by Sec proteins that drive vesicle budding from the endoplasmic reticulum. Cell 77, 895–907.

Barlowe C. (1997). Coupled ER to Golgi transport reconstituted with purified cytosolic proteins. J Cell Biol 139, 1097–108.

Behnia R, Barr FA, Flanagan JJ, Barlowe C, Munro S (2007). The yeast orthologue of GRASP65 forms a complex with a coiled-coil protein that contributes to ER to Golgi traffic. J Cell Biol 176, 255–261.

Belden WJ, Barlowe C (1996). Erv25p, a component of COPII-coated vesicles, forms a complex with Emp24p that is required for efficient endoplasmic reticulum to Golgi transport. J Biol Chem 271, 26939–26946.

Belden WJ, Barlowe C (2001). Distinct roles for the cytoplasmic tail sequences of Emp24p and Erv25p in transport between the endoplasmic reticulum and Golgi complex. J Biol Chem 276, 43040–43048.

Bhave M, Papanikou E, Iyer P, Pandya K, Jain BK, Ganguly A, Sharma C, Pawar K, Austin J 2nd, Day KJ, *et al.* (2014). Golgi enlargement in Arf-depleted yeast cells is due to altered dynamics of cisternal maturation. J Cell Sci 127, 250–257.

Bock JB, Matern HT, Peden AA, Scheller RH (2001). A genomic perspective on membrane compartment organization. Nature 409, 839–841.

Brachmann CB, Davies A, Cost GJ, Caputo E, Li J, Hieter P, Boeke JD (1998). Designer deletion strains derived from Saccharomyces cerevisiae S288C: a useful set of strains and plasmids for PCR-mediated gene disruption and other applications. Yeast 14, 115–132.

Brandizzi F, Barlowe C (2013). Organization of the ER-Golgi interface for membrane traffic control. Nat Rev Mol Cell Biol 14, 382–392.

Brigance WT, Barlowe C, Graham TR (2000). Organization of the yeast Golgi complex into at least four functionally distinct compartments. Mol Biol Cell 11, 171–182.

Brodsky JL, Schekman R (1993). A Sec63p-BiP complex from yeast is required for protein translocation in a reconstituted proteoliposome. J Cell Biol 123, 1355–1363.

Bruinsma P, Spelbrink RG, Nothwehr SF (2004). Retrograde transport of the mannosyltransferase Och1p to the early Golgi requires a component of the COG transport complex. J Biol Chem 279, 39814–39823.

Bue CA, Barlowe C (2009). Molecular dissection of Erv26p identifies separable cargo binding and coat protein sorting activities. J Biol Chem 284, 24049–24060.
Bue CA, Bentivoglio CM, Barlowe C (2006). Erv26p directs pro-alkaline phosphatase into endoplasmic reticulum-derived coat protein complex II transport vesicles. Mol Biol Cell 17, 4780–4789.
Cai H, Reinisch K, Ferro-Novick S (2007). Coats, tethers, Rabs, and SNAREs work together to mediate the intracellular destination of a transport vesicle. Dev Cell 12, 671–682.
Cancino J, Capalbo A, Di Campli A, Giannotta M, Rizzo R, Jung JE, Di Martino R, Persico M, Heinklein P, Sallese M, *et al*. (2014). Control systems of membrane transport at the interface between the endoplasmic reticulum and the Golgi. Dev Cell 30, 280–294.
Cao X, Ballew N, Barlowe C (1998). Initial docking of ER-derived vesicles requires Uso1p and Ypt1p but is independent of SNARE proteins. EMBO J 17, 2156–2165.
Climer LK, Dobretsov M, Lupashin V (2015). Defects in the COG complex and COG-related trafficking regulators affect neuronal Golgi function. Front Neurosci 9, 405.
Drin G, Morello V, Casella JF, Gounon P, Antonny B (2008). Asymmetric tethering of flat and curved lipid membranes by a golgin. Science 320, 670–673.
Fankhauser C, Conzelmann A (1991). Purification, biosynthesis and cellular localization of a major 125-kDa glycophosphatidylinositol-anchored membrane glycoprotein of Saccharomyces cerevisiae. Eur J Biochem 195, 439–448.
Feldheim D, Rothblatt J, Schekman R (1992). Topology and functional domains of Sec63p, an endoplasmic reticulum membrane protein required for secretory protein translocation. Mol Cell Biol 12, 3288–3296.
Fisher P, Ungar D (2016). Bridging the gap between glycosylation and vesicle traffic. Front Cell Dev Biol 4, 15.
Fridmann-Sirkis Y, Siniossoglou S, Pelham HR (2004). TMF is a golgin that binds Rab6 and influences Golgi morphology. BMC Cell Biol 5, 18.
Garrett MD, Zahner JE, Cheney CM, Novick PJ (1994). GDI1 encodes a GDP dissociation inhibitor that plays an essential role in the yeast secretory pathway. EMBO J 13, 1718–28.
Gillingham AK, Munro S (2016). Finding the Golgi: Golgin coiled-coil proteins whow the way. Trends Cell Biol 26, 399–408.
Gillingham AK, Pfeifer AC, Munro S (2002). CASP, the alternatively spliced product of the gene encoding the CCAAT-displacement protein transcription factor, is a Golgi membrane protein related to giantin. Mol Biol Cell 13, 3761–3774.
Gillingham AK, Tong AH, Boone C, Munro S (2004). The GTPase Arf1p and the ER to Golgi cargo receptor Erv14p cooperate to recruit the golgin Rud3p to the cis-Golgi. J Cell Biol 167, 281–292.
Ha JY, Chou HT, Ungar D, Yip CK, Walz T, Hughson FM (2016). Molecular architecture of the complete COG tethering complex. Nat Struct Mol Biol 23, 758–760.
Harris SL, Waters MG (1996). Localization of a yeast early Golgi mannosyltransferase, Och1p, involves retrograde transport. J Cell Biol 132, 985–998.
Hasilik A, Tanner W (1978). Carbohydrate moiety of carboxypeptidase Y and perturbation of its biosynthesis. Eur J Biochem 91, 567–575.
Heidtman M, Chen CZ, Collins RN, Barlowe C (2003). A role for Yip1p in COPII vesicle biogenesis. J Cell Biol 163, 57–69.
Hentges P, Van Driessche B, Tafforeau L, Vandenhaute J, Carr AM (2005). Three novel antibiotic marker cassettes for gene disruption and marker switching in Schizosaccharomyces pombe. Yeast 22, 1013–1019.
Holt LJ, Tuch BB, Villen J, Johnson AD, Gygi SP, Morgan DO (2009). Global analysis of Cdk1 substrate phosphorylation sites provides insights into evolution. Science 325, 1682–1686.
Inadome H, Noda Y, Adachi H, Yoda K (2005). Immunoisolaton of the yeast Golgi subcompartments and characterization of a novel membrane protein, Svp26, discovered in the Sed5-containing compartments. Mol Cell Biol 25, 7696–7710.
Ito H, Fukuda Y, Murata K, Kimura A (1983). Transformation of intact yeast cells treated with alkali cations. J Bacteriol 153, 163–168.
Kaiser CA, Schekman R (1990). Distinct sets of SEC genes govern transport vesicle formation and fusion early in the secretory pathway. Cell 61, 723–733.
Kim DW (2003). Characterization of Grp1p, a novel cis-Golgi matrix protein. Biochem Biophys Res Commun 303, 370–378.
Kim DW, Sacher M, Scarpa A, Quinn AM, Ferro-Novick S (1999). High-copy suppressor analysis reveals a physical interaction between Sec34p and Sec35p, a protein implicated in vesicle docking. Mol Biol Cell 10, 3317–3329.
Lanoix J, Ouwendijk J, Stark A, Szafer E, Cassel D, Dejgaard K, Weiss M, Nilsson T (2001). Sorting of Golgi resident proteins into different subpopulations of COPI vesicles: a role for ArfGAP1. J Cell Biol 155, 1199–1212.
Laufman O, Kedan A, Hong W, Lev S (2009). Direct interaction between the COG complex and the SM protein, Sly1, is required for Golgi SNARE pairing. EMBO J 28, 2006–2017.
Lees JA, Yip CK, Walz T, Hughson FM (2010). Molecular organization of the COG vesicle tethering complex. Nat Struct Mol Biol 17, 1292–1297.
Levi SK, Bhattacharyya D, Strack RL, Austin JR 2nd, Glick BS (2010). The yeast GRASP Grh1 colocalizes with COPII and is dispensable for organizing the secretory pathway. Traffic 11, 1168–79.
Lipschutz JH, Lingappa VR, Mostov KE (2003). The exocyst affects protein synthesis by acting on the translocation machinery of the endoplasmic reticulum. J Biol Chem 278, 20954–20960.
Liu G, Yong MY, Yurieva M, Srinivasan KG, Liu J, Lim JS, Poidinger M, Wright GD, Zolezzi F, Choi H, *et al*. (2015). Gene essentiality is a quantitative property linked to cellular evolvability. Cell 163, 1388–1399.
Longtine MS, McKenzie A 3rd, Demarini DJ, Shah NG, Wach A, Brachat A, Philippsen P, Pringle JR (1998). Additional modules for versatile and economical PCR-based gene deletion and modification in Saccharomyces cerevisiae. Yeast 14, 953–961.
Luini A, Mavelli G, Jung J, Cancino J (2014). Control systems and coordination protocols of the secretory pathway. F1000Prime Rep 6, 88.
Malsam J, Satoh A, Pelletier L, Warren G (2005). Golgin tethers define subpopulations of COPI vesicles. Science 307, 1095–1098.
Margulis NG, Wilson JD, Bentivoglio CM, Dhungel N, Gitler AD, Barlowe C (2016). Analysis of COPII vesicles indicates a role for the Emp47-Ssp120 complex in transport of cell surface glycoproteins. Traffic 17, 191–210.
Martinez-Menarguez JA, Prekeris R, Oorschot VM, Scheller R, Slot JW, Geuze HJ, Klumperman J (2001). Peri-Golgi vesicles contain retrograde but not anterograde proteins consistent with the cisternal progression model of intra-Golgi transport. J Cell Biol 155, 1213–1224.
Merz AJ, Wickner WT (2004). Trans-SNARE interactions elicit Ca2+ efflux from the yeast vacuole lumen. J Cell Biol 164, 195–206.
Miller VJ, Sharma P, Kudlyk TA, Frost L, Rofe AP, Watson IJ, Duden R, Lowe M, Lupashin VV, Ungar D (2013). Molecular insights into vesicle tethering at the Golgi by the conserved oligomeric Golgi (COG) complex and the golgin TATA element modulatory factor (TMF). J Biol Chem 288, 4229–4240.
Mizuno-Yamasaki E, Rivera-Molina F, Novick P (2012). GTPase networks in membrane traffic. Annu Rev Biochem 81, 637–659.
Mizuta K, Warner JR (1994). Continued functioning of the secretory pathway is essential for ribosome synthesis. Mol Cell Biol 14, 2493–2502.
Mukherjee I, Barlowe C (2016). Overexpression of Sly41 suppresses COPII vesicle-tethering deficiencies by elevating intracellular calcium levels. Mol Biol Cell 27, 1635–1649.
Munro S. (2011). The golgin coiled-coil proteins of the Golgi apparatus. Cold Spring Harb Perspect Biol 3, a005256.
Nakanishi-Shindo Y, Nakayama K, Tanaka A, Toda Y, Jigami Y (1993). Structure of the N-linked oligosaccharides that show the complete loss of alpha-1,6-polymannose outer chain from och1, och1 mnn1, and och1 mnn1 alg3 mutants of Saccharomyces cerevisiae. J Biol Chem 268, 26338–26345.
Otte S, Belden WJ, Heidtman M, Liu J, Jensen ON, Barlowe C (2001). Erv41p and Erv46p: new components of COPII vesicles involved in transport between the ER and Golgi complex. J Cell Biol 152, 503–518.
Papanikou E, Day KJ, Austin J, Glick BS (2015). COPI selectively drives maturation of the early Golgi. Elife 4, e13232.
Parlati F, McNew JA, Fukuda R, Miller R, Sollner TH, Rothman JE (2000). Topological restriction of SNARE-dependent membrane fusion. Nature 407, 194–198.
Parlati F, Varlamov O, Paz K, McNew JA, Hurtado D, Sollner TH, Rothman JE (2002). Distinct SNARE complexes mediating membrane fusion in Golgi transport based on combinatorial specificity. Proc Natl Acad Sci USA 99, 5424–5429.
Peng R, Gallwitz D (2002). Sly1 protein bound to Golgi syntaxin Sed5p allows assembly and contributes to specificity of SNARE fusion complexes. J Cell Biol 157, 645–655.
Powers J, Barlowe C (1998). Transport of axl2p depends on erv14p, an ER-vesicle protein related to the Drosophila cornichon gene product. J Cell Biol 142, 1209–1222.
Puthenveedu MA, Bachert C, Puri S, Lanni F, Linstedt AD (2006). GM130 and GRASP65-dependent lateral cisternal fusion allows uniform Golgi-enzyme distribution. Nat Cell Biol 8, 238–248.

Ram AF, Wolters A, Ten Hoopen R, Klis FM (1994). A new approach for isolating cell wall mutants in Saccharomyces cerevisiae by screening for hypersensitivity to calcofluor white. Yeast 10, 1019–1030.
Ren Y, Yip CK, Tripathi A, Huie D, Jeffrey PD, Walz T, Hughson FM (2009). A structure-based mechanism for vesicle capture by the multisubunit tethering complex Dsl1. Cell 139, 1119–1129.
Roboti P, Sato K, Lowe M (2015). The golgin GMAP-210 is required for efficient membrane trafficking in the early secretory pathway. J Cell Sci 128, 1595–1606.
Rothblatt JA, Deshaies RJ, Sanders SL, Daum G, Schekman R (1989). Multiple genes are required for proper insertion of secretory proteins into the endoplasmic reticulum in yeast. J Cell Biol 109, 2641–2652.
Salama NR, Yeung T, Schekman RW (1993). The Sec13p complex and reconstitution of vesicle budding from the ER with purified cytosolic proteins. EMBO J 12, 4073–4082.
Seemann J, Jokitalo E, Pypaert M, Warren G (2000). Matrix proteins can generate the higher order architecture of the Golgi apparatus. Nature 407, 1022–1026.
Shestakova A, Suvorova E, Pavliv O, Khaidakova G, Lupashin V (2007). Interaction of the conserved oligomeric Golgi complex with t-SNARE Syntaxin5a/Sed5 enhances intra-Golgi SNARE complex stability. J Cell Biol 179, 1179–1192.
Shibuya A, Margulis N, Christiano R, Walther TC, Barlowe C (2015). The Erv41-Erv46 complex serves as a retrograde receptor to retrieve escaped ER proteins. J Cell Biol 208, 197–209.
Siniossoglou S (2005). Affinity purification of Ypt6 effectors and identification of TMF/ARA160 as a Rab6 interactor. Methods Enzymol 403, 599–607.
Siniossoglou S, Pelham HR (2001). An effector of Ypt6p binds the SNARE Tlg1p and mediates selective fusion of vesicles with late Golgi membranes. EMBO J 20, 5991–5998.
Spang A, Schekman R (1998). Reconstitution of retrograde transport from the Golgi to the ER in vitro. J Cell Biol 143, 589–599.
Stanley P (2011). Golgi glycosylation. Cold Spring Harb Perspect Biol 3, a005199.
Stevens T, Esmon B, Schekman R (1982). Early stages in the yeast secretory pathway are required for transport of carboxypeptidase Y to the vacuole. Cell 30, 439–448.
Suvorova ES, Duden R, Lupashin VV (2002). The Sec34/Sec35p complex, a Ypt1p effector required for retrograde intra-Golgi trafficking, interacts with Golgi SNAREs and COPI vesicle coat proteins. J Cell Biol 157, 631–643.
Swaney DL, Beltrao P, Starita L, Guo A, Rush J, Fields S, Krogan NJ, Villen J (2013). Global analysis of phosphorylation and ubiquitylation cross-talk in protein degradation. Nat Methods 10, 676–682.
Tai G, Lu L, Wang TL, Tang BL, Goud B, Johannes L, Hong W (2004). Participation of the syntaxin 5/Ykt6/GS28/GS15 SNARE complex in transport from the early/recycling endosome to the trans-Golgi network. Mol Biol Cell 15, 4011–4022.
Thorngren N, Collins KM, Fratti RA, Wickner W, Merz AJ (2004). A soluble SNARE drives rapid docking, bypassing ATP and Sec17/18p for vacuole fusion. EMBO J 23, 2765–2776.
Todorow Z, Spang A, Carmack E, Yates J, Schekman R (2000). Active recycling of yeast Golgi mannosyltransferase complexes through the endoplasmic reticulum. Proc Natl Acad Sci USA 97, 13643–13648.
Toikkanen JH, Miller KJ, Soderlund H, Jantti J, Keranen S (2003). The beta subunit of the Sec61p endoplasmic reticulum translocon interacts with the exocyst complex in Saccharomyces cerevisiae. J Biol Chem 278, 20946–20953.
Tong AH, Evangelista M, Parsons AB, Xu H, Bader GD, Pagé N, Robinson M, Raghibizadeh S, Hogue CW, Bussey H, *et al.* (2001). Systematic genetic analysis with ordered arrays of yeast deletion mutants. Science 294, 2364–2368.
Tong AH, Boone C (2006). Synthetic genetic array analysis in Saccharomyces cerevisiae. Methods Mol Biol 313, 171–192.
Tsui MM, Banfield DK (2000). Yeast Golgi SNARE interactions are promiscuous. J Cell Sci 113, 145–152.
Tsui MM, Tai WC, Banfield DK (2001). Selective formation of Sed5p-containing SNARE complexes is mediated by combinatorial binding interactions. Mol Biol Cell 12, 521–538.
Tu L, Tai WC, Chen L, Banfield DK (2008). Signal-mediated dynamic retention of glycosyltransferases in the Golgi. Science 321, 404–407.
Ungermann C, Sato K, Wickner W (1998). Defining the functions of trans-SNARE pairs. Nature 396, 543–548.
VanRheenen SM, Cao X, Lupashin VV, Barlowe C, Waters MG (1998). Sec35p, a novel peripheral membrane protein, is required for ER to Golgi vesicle docking. J Cell Biol 141, 1107–1119.
VanRheenen SM, Cao X, Sapperstein SK, Chiang EC, Lupashin VV, Barlowe C, Waters MG (1999). Sec34p, a protein required for vesicle tethering to the yeast Golgi apparatus, is in a complex with Sec35p. J Cell Biol 147, 729–742.
Volchuk A, Ravazzola M, Perrelet A, Eng WS, Di Liberto M, Varlamov O, Fukasawa M, Engel T, Söllner TH, Rothman JE, *et al.* (2004). Countercurrent distribution of two distinct SNARE complexes mediating transport within the Golgi stack. Mol Biol Cell 15, 1506–1518.
Willett R, Kudlyk T, Pokrovskaya I, Schonherr R, Ungar D, Duden R, Lupashin V (2013). COG complexes form spatial landmarks for distinct SNARE complexes. Nat Commun 4, 1553.
Wilson JD, Barlowe C (2010). Yet1p and Yet3p, the yeast homologs of BAP29 and BAP31, interact with the endoplasmic reticulum translocation apparatus and are required for inositol prototrophy. J Biol Chem 285, 18252–18261.
Witkos TM, Lowe M (2015). The Golgin Family of Coiled-Coil Tethering Proteins. Front Cell Dev Biol 3, 86.
Wong M, Munro S (2014). Membrane trafficking. The specificity of vesicle traffic to the Golgi is encoded in the golgin coiled-coil proteins. Science 346, 1256898.
Wooding S, Pelham HR (1998). The dynamics of golgi protein traffic visualized in living yeast cells. Mol Biol Cell 9, 2667–2680.
Wuestehube LJ, Duden R, Eun A, Hamamoto S, Korn P, Ram R, Schekman R (1996). New mutants of Saccharomyces cerevisiae affected in the transport of proteins from the endoplasmic reticulum to the Golgi complex. Genetics 142, 393–406.
Wuestehube LJ, Schekman RW (1992). Reconstitution of transport from endoplasmic reticulum to Golgi complex using endoplasmic reticulum-enriched membrane fraction from yeast. Methods Enzymol 219, 124–136.
Xu C, Ng DT (2015). Glycosylation-directed quality control of protein folding. Nat Rev Mol Cell Biol 16, 742–752.
Xu Y, Martin S, James DE, Hong W (2002). GS15 forms a SNARE complex with syntaxin 5, GS28, and Ykt6 and is implicated in traffic in the early cisternae of the Golgi apparatus. Mol Biol Cell 13, 3493–3507.
Yu IM, Hughson FM (2010). Tethering factors as organizers of intracellular vesicular traffic. Annu Rev Cell Dev Biol 26, 137–156.
Zink S, Wenzel D, Wurm CA, Schmitt HD (2009). A link between ER tethering and COP-I vesicle uncoating. Dev Cell 17, 403–416.
Zolov SN, Lupashin VV (2005). Cog3p depletion blocks vesicle-mediated Golgi retrograde trafficking in HeLa cells. J Cell Biol 168, 747–759.